

**Altering the targeting specificity of rocaglates: selective
eIF4A inhibitors**

Kesha Patel

Department of Biochemistry,
McGill University, Montreal

November 2022

A thesis submitted to McGill University in partial fulfillment of the requirements of the degree of Master of Science.

© Kesha Patel 2022

ABSTRACT

DEAD-box RNA helicases are the family of putative RNA helicases with 37 members in mammals and are characterized by the presence of a highly conserved Asp-Glu-Ala-Asp (DEAD) motif. DDX proteins are key players in all facets of RNA biology ranging from transcription to mRNA decay. However, the specific functions of most DDX helicases in various cellular processes are largely unknown. Dysregulation of these helicases has been associated with tumor cell maintenance. In light of this fact, significant efforts have been made over the years in developing small molecules against DEAD-box proteins to understand their role in physiological processes and the possibility of targeting these in various malignancies. DDX helicases have a structurally highly conserved core with various N-terminal and C-terminal flanking ends that determine their substrate specificity and function. Of all RNA helicases, eIF4A (DDX2) is the smallest and best characterized DEAD-box RNA helicase. It is a prototype of DDX helicases that plays a crucial role in translation initiation. Our lab studies three natural small molecule inhibitors targeting eIF4A, of which rocaglates are the best characterized, are potent and well-tolerated *in vivo*. Rocaglates clamp eIF4A onto the purine rich regions of RNA and inhibit global translation by blocking the ribosomal scanning towards the start codon and inhibiting the recruitment of 40S ribosome onto the RNA. They exert their effect by wedging themselves between two RNA bases and interacting with F163 and Q195 of eIF4A. Only DDX2 paralogs have F163 and Q195 residues at these positions, whereas other DEAD-box proteins have distinct residues at these key interacting positions. Taking this into an account and that the helicase core is highly conserved, we hypothesized that these helicases could be targeted by slightly modifying rocaglates at eIF4A1 interacting sites. Using structure-based drug design and chemical biology approach, we modified rocaglates to explore the possibility of broadening their

targeting spectrum from selective eIF4A inhibitors to various DEAD-box proteins and target these helicases in cancers.

RÉSUMÉ

Les protéines de la famille des hélicases à ARN de type « DEAD-box » comptent 37 membres putatifs chez les mammifères et se caractérisent par la présence du motif Asp-Glu-Ala-Asp (DEAD). Ces protéines jouent un rôle essentiel dans toutes les facettes de la biologie de l'ARN, de la transcription jusqu'à la dégradation des ARN messagers (ARNm). Cependant, les fonctions spécifiques de la grande majorité des hélicases de type « DEAD-box » dans les procédés biologiques restent encore méconnues. Le dérèglement de l'activité de ces hélicases a été associé au maintien phénotypique des cellules cancéreuses. Afin de contrer ces lacunes, plusieurs efforts ont été faits au courant des dernières années pour développer des inhibiteurs moléculaires pouvant cibler les hélicases de type « DEAD-box » dans un but thérapeutique, mais aussi pour mieux comprendre leur rôle physiologique. Ces enzymes possèdent un noyau structurellement très conservé avec différentes extrémités N et C terminales qui déterminent la spécificité du substrat et leur fonction. De toutes ces hélicases, eIF4A (DDX2) est la plus petite, mais aussi la mieux caractérisée. Elle joue un rôle crucial dans l'initiation de la traduction des ARNm. Au laboratoire, nous étudions présentement trois molécules ciblant eIF4A, dont les rocaglates qui sont les mieux caractérisés et qui sont bien tolérés *in vivo*. Les rocaglates fixent eIF4A sur les régions riches en purines de l'ARN et inhibent la traduction globale en bloquant le balayage des ribosomes vers le codon d'initiation et en inhibant le recrutement de la sous-unité ribosomique 40S sur l'ARNm. Ils exercent leur effet en se calant entre deux bases d'ARN et en interagissant avec F163 et Q195 d'eIF4A. Seuls les paralogues de eIF4A possèdent des résidus F163 et Q195 à ces positions, les autres protéines de type « DEAD-box » ayant des résidus distincts à ces positions clés. Compte tenu de ceci et du fait que le noyau de l'hélicase est hautement conservé génétiquement, nous avons émis l'hypothèse que les autres hélicases pourraient être ciblées en modifiant légèrement la structure des rocaglates au site d'interaction avec

eIF4A1. En utilisant la conception de médicaments basée sur la structure et l'approche de la biologie chimique, nous avons modifié les rocaglates pour explorer la possibilité d'élargir leur spectre de ciblage à diverses protéines de type « DEAD-box » afin de cibler ces hélicases dans le cancer.

ACKNOWLEDGEMENTS

First and foremost, I would like to thank my supervisor, Dr. Jerry Pelletier, for giving me an opportunity to work under his guidance. I am extremely grateful to have had a supervisor who was very much invested in the project and was always available to discuss results or new ideas for the project. Jerry's determination and discipline for science have always inspired me to push myself beyond my limits.

I would like to extend my thanks to all the lab members of the Pelletier lab who guided me throughout my academic journey. Special thanks to Sai Kiran Naineni who mentored me ever since I started working in this lab. He has provided me invaluable guidance throughout my masters and has added to my knowledge in the project. Thank you for always being patient while answering all my questions, for providing ideas for the project, and for helping me in interpreting results. A big thank you to Dr. Francis Robert for sharing his expertise in molecular cloning and helping me solve problems with the same; Lauren, for being an amazing bench-mate and a good friend who also provided moral support; Samer, for being a great companion with whom I have also had long discussions about both science and life; Pushkarni, for being a great friend; Jordan, Aamir, Round and Web who I am happy to have met. I am also thankful to Dr. Regina Cencic for training me with all the tissue culture work. Many thanks to Patrick for placing all the orders for my project; Sophia, for giving a homely touch to the lab during festivals, and for always being so kind and considerate.

I would also like to thank my Research Advisory Committee members, Dr. Sidong Huang and Dr. Imed Gallouzi for providing constructive feedback on the project. Additionally, I would like to extend my

thanks to our collaborators Dr. John Porco and Dr. Lauren Brown to provide us with the compound library without which this thesis would not have been possible. I'd like to acknowledge Ms. Christine Laberge for all the administrative help in these two years.

Lastly, to my parents, my lovely siblings, and friends, thank you very much for your unwavering support. I would not have been able to do this without your emotional support.

CONTRIBUTION OF AUTHORS

The entire thesis is written by the author. All the experiments and data analysis presented herein were performed by the author. The experiments were planned by Dr. Jerry Pelletier, Mr. Sai Kiran Naineni and the author. Original idea of the project was conceived and planned by Dr. Jerry Pelletier, and he supervised the project.

TABLE OF CONTENTS

ABSTRACT.....	2
RÉSUMÉ.....	4
ACKNOWLEDGEMENTS.....	6
CONTRIBUTION OF AUTHORS.....	8
LIST OF FIGURES.....	11
LIST OF TABLES.....	12
LIST OF ABBREVIATIONS.....	13
1. INTRODUCTION.....	17
1.1 Helicases.....	17
1.2 DEAD-box RNA Helicases.....	18
1.2.1 Structural components of DEAD-box RNA helicases.....	18
1.2.2 Functions of DEAD-box RNA helicases.....	21
1.3 Protein Synthesis.....	24
1.3.1 Cap-dependent translation initiation.....	25
1.3.2 The eIF4F complex.....	28
1.4 Targeting DEAD-box RNA helicases as therapeutic vulnerabilities in cancer.....	31
1.5 Small molecule inhibitors of DEAD-box RNA helicases... ..	33
1.5.1 DDX2 (eIF4A)	33
1.5.2 DDX3X	39
1.5.3 DDX5	39
1.5.4 DDX48.....	40
1.6 Overview and rationale for the thesis.....	41
2. MATERIAL AND METHODS.....	43
2.1 General materials.....	43
2.2 Compounds.....	43
2.3 Construction of expression vectors.....	43
2.4 Expression and purification of recombinant proteins.....	43
2.5 ATPase assay.....	44
2.6 Fluorescence polarization assay.....	45

3. RESULTS.....	46
3.1 Qualitative assessment of engineered recombinant proteins.....	46
3.2 Functional analysis of the wild-type and recombinant eIF4A1 proteins.....	49
3.3 CR-1-31-B stimulates clamping of recombinant proteins onto poly (AG) ₈ RNA.....	52
3.4 Comparative assessment of rocaglate mediated WT/ mutant -eIF4A1: RNA clamping.....	54
4. DISCUSSION	66
5. CONCLUSION.....	74
REFERENCES.....	75

LIST OF FIGURES

Figure 1. The DEAD-box RNA helicase family.

Figure 2. Schematic diagram showing DEAD-box proteins involved in various cellular processes.

Figure 3. Overview of cap-dependent eukaryotic translation initiation.

Figure 4. Assembly of eIF4F complex and its role in translation initiation.

Figure 5. Small molecule inhibitors of eIF4A.

Figure 6. Structural basis of rocaglate binding to eIF4A1.

Figure 7. Strategy to target a specific DEAD-box RNA helicase.

Figure 8. Recombinant protein engineering.

Figure 9. Assessment of ATP hydrolysis by purified proteins via Thin Layer Chromatography (TLC).

Figure 10. Quantitation of kinetics of ATP hydrolysis by the purified recombinant proteins.

Figure 11. Measuring CR-1-31-B mediated RNA binding of purified proteins.

Figure 12. Protein titrations to fix the working concentration in FP assay.

Figure 13. Measuring eIF4A1 mutants:FAM- poly (AG)₈ RNA binding by rocaglates using FP assay.

Figure 14. Comparative evaluation of rocaglates stimulated RNA binding of wt eIF4A1 vs mutant eIF4A1.

Figure 15. Structural basis for potential interactions between rocaglates and D198R mutant.

Figure 16. Rocaglates showing promiscuous activity in clamping assay.

Figure 17. Rocaglates exhibiting specificity towards eIF4A1 mutants.

LIST OF TABLES

Table 1. Amino acid diversity in mammalian DEAD-box helicases corresponding to positions 163 and 195 of eIF4A1 and the properties of these residues.

LIST OF ABBREVIATIONS

Δ mP	Change in polarization
4E-BPs	eIF4E- Binding Protein
4EHP	eIF4E Homologous Protein
AMP-PNP	Adenylyl-Imidodiphosphate
ARF	Alternative Reading Frame
ATP	Adenosine Triphosphate
Bcl2	B-Cell Lymphoma-2
BU-CMD	Boston University- Center for Molecular Discovery
cDNA	Complementary Deoxyribonucleic Acid
CHX	Cycloheximide
CRM1	Chromosomal Maintenance 1
CTD	C-Terminal Domain
DMSO	Dimethyl sulfoxide
DNA	Deoxyribonucleic Acid
DTT	Dithiothreitol
EDG	Electron Donating Group
EDTA	Ethylenediaminetetraacetic acid
eIF	Eukaryotic Initiation Factor
EJC	Exon- Junction Complex
eRF3	Eukaryotic Polypeptide Chain Releasing Factor 3
FAM	Fluorescein Amidite

FP	Fluorescence Polarization
FPA	Fluorescence Polarization Assay
GDP	Guanosine Diphosphate
GTP	Guanosine Triphosphate
HCV	Hepatitis C Virus
HEAT	Huntingtin, Elongation Factor 3, Protein Phosphatase 2A, Tor1 Repeat Structure
heIF	human Eukaryotic Initiation Factor
HHT	Homoharringtonine
HNSCC	Head and Neck Squamous Cell Carcinoma
IP ₆	Inositol hexaphosphate
IPTG	Isopropyl β- d-1-Thiogalactopyranoside
LTM	Lactimidomycin
Met-tRNA _i	Methionine Initiator Transfer Ribonucleic Acid
miRNA	Micro RNA
MM	Multiple Myeloma
MNK	MAP Kinase Interacting Kinase
mP	Polarization value
mRNA	Messenger Ribonucleic Acid
mRNP	Messenger Ribonucleoprotein
mTORC1	Mammalian Target of Rapamycin Complex 1
Ni:NTA	Nickel (II) Nitriloacetate
NMD	Nonsense Mediated Decay

NMR	Nuclear Magnetic Resonance
NSCLC	Non-Small-Cell Lung Carcinoma
NTD	N-Terminal Domain
NTP	Nucleoside Triphosphate
NS3	Nonstructural Protein 3
nts	Nucleotides
PABP	Poly(A) Binding Protein
PDCD4	Programmed Cell Death 4
PIC	Pre-Initiation Complex
PIEDA	Pair Interaction Energy Decomposition Analysis
PTC	Premature Termination Codon
RECQL4	RecQ Like Helicase 4
REN	Ring Expanding Nucleosides
RHT	Rohitinib
RNA	Ribonucleic Acid
rRNA	Ribosomal RNA
RTS	Rothmund-Thomson Syndrome
SF	Superfamily
snRNP	Small Nuclear Ribonucleoprotein
snoRNA	Small Nucleolar RNAs
ssRNA	Single Stranded RNA
TC	Ternary Complex
TISU	Translation Initiator of Short 5'UTR

TLC	Thin Layer Chromatography
UTR	Untranslated Region
WT	Wild-Type
XRN1	Exoribonuclease 1

1. INTRODUCTION

1.1 Helicases

Helicases are enzymes that bind or remodel nucleic acids, nucleic-acid protein complexes, or both by utilizing the energy derived from NTP hydrolysis [1-3]. They are one of the largest classes of enzymes encoded by all cellular life forms, along with viruses [4, 5]. Based on amino acid sequence, structure, and function, helicases are classified into six superfamilies (SFs) [3, 6]. All the ring-forming helicases are categorized under SFs 3 to 6, whereas the non-ring-forming ones belong to SFs 1 and 2 [3]. The ring-forming helicases form a hexameric core containing six individual domains arranged in a ring structure. In comparison, the enzymes in SF 1 and 2 have a core with two domains that are connected by a linker region. These domains are known as RecA- like domains since they share a resemblance with the ATP-binding core of bacterial recombinase A (RecA) [3, 7]. Based on their substrate specificity, helicases are categorized as either DNA or RNA helicases. Apart from these, some helicases like HCV protease NS3 are bifunctional and can target both DNA and RNA duplexes [8], whereas a few can unwind DNA-RNA duplexes [9, 10]. SF 1 and 2 are the largest helicase superfamilies comprising both DNA and RNA helicases. All eukaryotic RNA helicases belong to SF 1 and SF2, and most of them belong to the DExD/H-box family of proteins in SF2 (Figure 1b). They are further classified into two families- the DEAD-box and DEAH-box families. They are named after the single-letter designation of amino acids (Asp-Glu-Ala-Asp/ His) present in the motif II of their helicase domain. However, the amino acid sequence varies in the other motifs of the helicase domain, which differentiates these two families [7].

1.2 DEAD-box RNA Helicases

DEAD-box RNA helicases are the largest group of helicases in the SF2 of helicase superfamily with more than 30 members in humans. They are conserved from bacteria and viruses to humans and carry a signature Asp-Glu-Ala-Asp (D-E-A-D) sequence in motif II that attributes to their name [11]. They are embroiled in all the facets of RNA metabolism starting from RNA biogenesis to mRNA decay. They play a central role in the rearrangement and remodeling of structural elements in RNA in an ATP-dependent manner [11-14].

1.2.1 Structural components of DEAD-box RNA helicases

All members in the DEAD-box family of proteins consist of a structurally highly conserved core of two RecA-like domains. Both these domains collectively contain twelve conserved motifs that are implicated in ATP binding and hydrolysis, RNA binding, and coordination between ATP-binding and RNA-binding regions (Figure 1c). These two domains are connected by a flexible linker region that forms two inter-domain clefts where resides an ATP-binding site. The RNA-binding site lies opposite to the ATP-binding site [3, 10, 15]. The ATP-binding site is scattered through both domains with motifs Q, I, II and VI being involved in the interaction. Nucleotide specificity for adenine is conferred by the highly conserved glutamine residue in the Q-motif [16-18]. Motifs Ia, Ib, Ic, IV, IVa, and V participate in interacting with ssRNA. Amino acid residues from motifs III and Va play a central role in interlinking both ATP and RNA interacting regions to facilitate ATP binding and hydrolysis followed by ATP-dependent RNA unwinding [3, 15, 19, 20]. In addition to the common core, various DEAD-box helicases contain varied N-terminal and C-terminal flanking ends that mediate substrate specificity [21]. For example, the DEAD-box protein YxiN in *Bacillus subtilis* contains an RNA recognition motif in the C-

terminus that binds to the hairpin structure of the 23S rRNA and presumably anchors the helicase on rRNA during ribosome biogenesis [21].

As two domains of the helicase core are connected via a flexible linker, DEAD-box RNA helicases can transition between inactive open and active closed conformations. In the absence of RNA and ATP, the two domains in the helicase core do not engage and adopt an open conformation. Upon the binding of these substrates, the helicase core adopts a compact closed conformation where most of the conserved motifs face towards each other at the interdomain cleft and are involved in hydrogen bonding. The ATP molecule is embedded at the bottom of the interdomain cleft and interacts with residues from both the domains. Likewise, RNA binds opposite to the ATP binding site over both the domains and stabilizes this complex into its active conformation [15, 22, 23]. The unwound RNA is then released which can be either coupled to ATP-binding in a few cases or ATP hydrolysis in the rest [24-26]. The RNA binding sites in the helicase core exclusively interact with the sugar-phosphate backbone of the RNA suggesting that DEAD-box helicases bind to RNA in a sequence-independent manner [27]. Owing to their lack of specificity for RNA sequences, they function as general RNA chaperones that target several RNAs [28, 29]. This modulation between open and closed conformations is substantial for the catalytic cycle of DEAD-box proteins. However, since DEAD-box proteins unwind RNA duplexes by clamping onto the same and separating the two strands, they can only unwind short RNA sequences up to 10-15 base pairs in length [26, 30, 31].

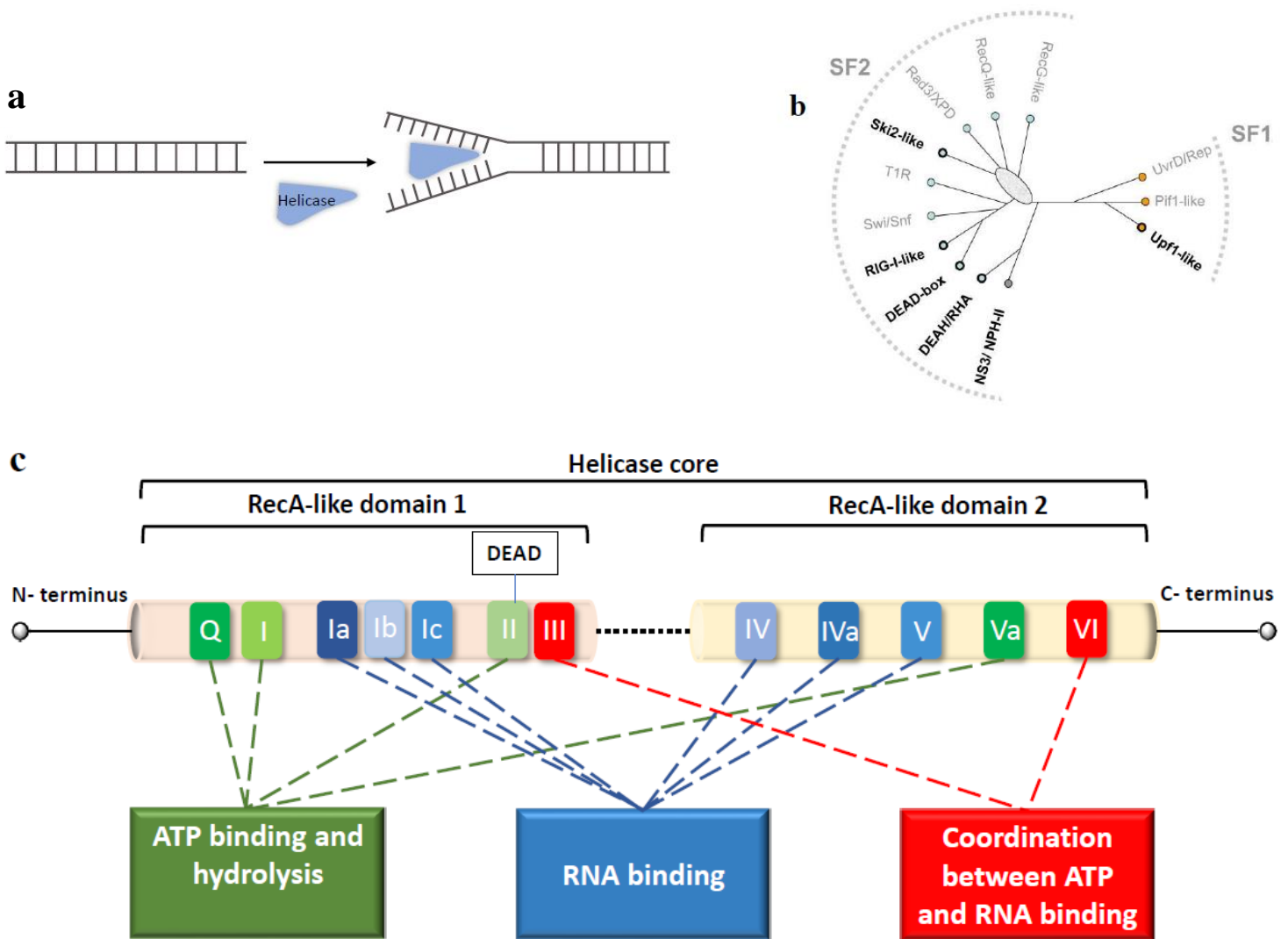


Figure 1. The DEAD-box RNA helicase family. (a) Schematic diagram showing the unwinding activity of helicase. (b) SF1 and SF2 helicase families. Boldfaced names represent the families harboring RNA helicases. The names in grey represent the families harboring DNA helicases. (c) Schematic representation showing conserved domains and motifs throughout DEAD-box RNA helicase family. The helicase core consists of two RecA-like domains and the conserved motifs in it are involved in ATP binding and hydrolysis (red), RNA binding (blue) and communication between ATP-binding and RNA-binding sites (green). Fig 1(b) taken from Ref. [10]. Fig 1(c) adapted from Ref. [15].

1.2.2 Functions of DEAD-box RNA helicases

DEAD-box proteins play a vital role in all the biological processes requiring RNA including transcription, pre-mRNA splicing, miRNA biogenesis, rRNA processing, ribosome biogenesis, RNA export, translation, and mRNA decay [15, 32]. Of these, only select processes in which DEAD-box proteins have been implicated and those proteins for which more data is available in the literature are described herein.

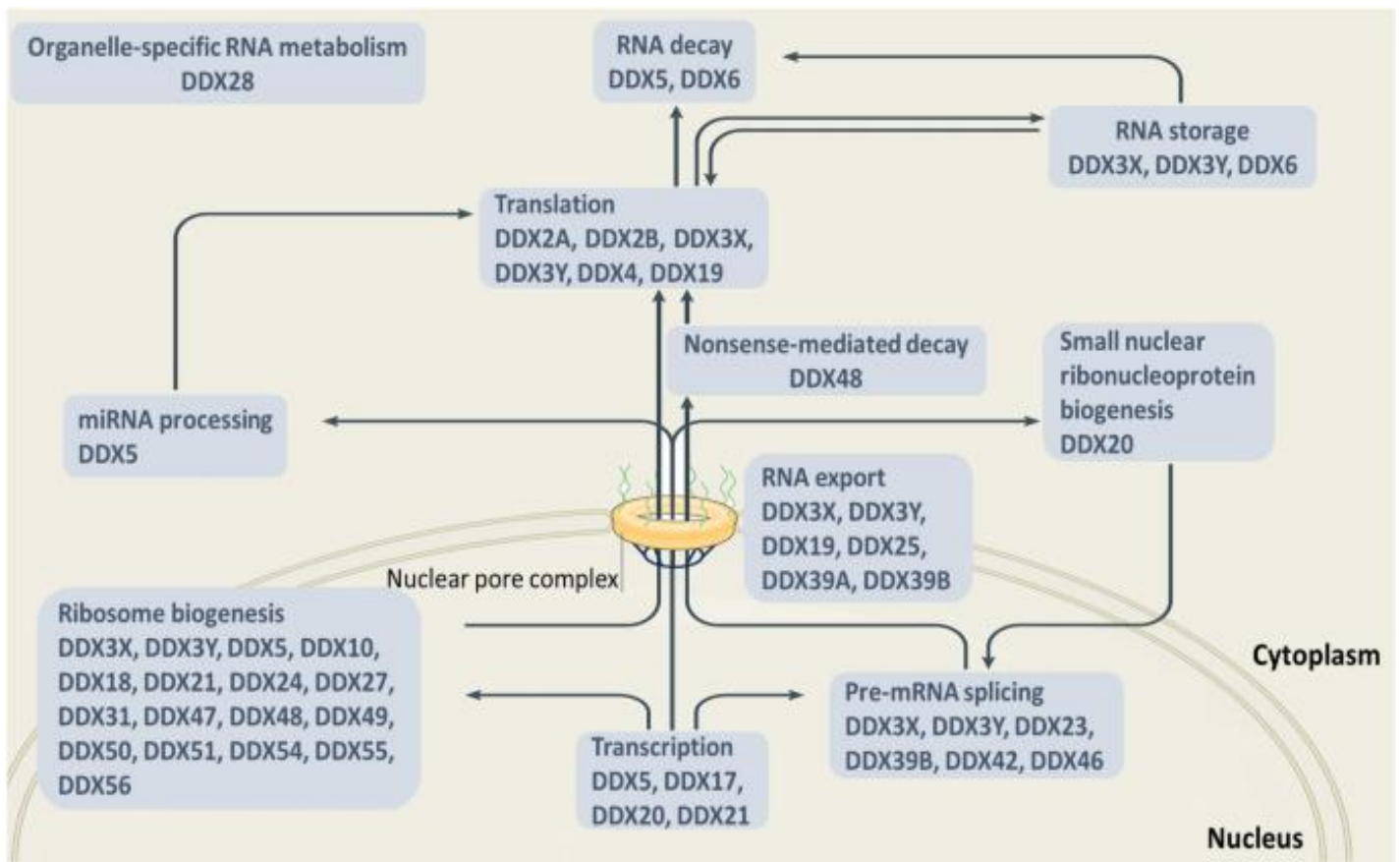


Figure 2. Schematic diagram showing DEAD-box proteins involved in various cellular processes. Figure obtained from Ref. [15].

DEAD-box proteins in nuclear processes

In the nucleus, some of the DEAD-box proteins interact with principal components of transcription machinery and play a vital role in regulating transcription. For instance, DDX5 acts as a transcriptional co-activator of p53 tumor suppressor protein [33, 34], steroid hormone receptor family including Vitamin D receptor, human estrogen receptor α and androgen receptor [35, 36]. Moreover, they are also reported to be overexpressed in glioma cells and other cancers [37, 38]. DDX5 and its paralog DDX17 both interact with histone deacetylases 1 and act as transcriptional repressors in a context dependent manner [39]. DDX21 regulates transcriptional and post-transcriptional steps of ribosome biogenesis by interacting with components of snRNP complexes and plays a significant role in tumor cell growth [40]. DDX41 has been shown to interact with spliceosome components and myeloid-associated mutations in this helicase influence alternative splicing [41, 42]. DDX48 plays a critical role in regulating alternative splicing events in mammals by affecting the rate of transcriptional elongation by Pol II [43]. DDX19B acts as a scaffolding protein that assists transportation of mRNPs from nucleus towards the cytoplasmic face of nuclear pore complex (NPC) [44]. Once at the NPC, DDX19B interacts with Gle 1, a DDX modulator that activates DDX19B in an IP_6 – dependent manner and releases the mRNP in the cytoplasm [45]. DDX39B recruits adaptor proteins like Aly/REF export factor to mRNP that are required to make the mRNA competent for nuclear transport [32]. Moreover, DDX3X has been shown to participate in exporting viral mRNA by binding with CRM1 (a nuclear export protein) through its C-terminal residues and localizing to nuclear membrane pores. Additionally, it has also been shown to associate with tip-associated protein (TAP), which is a major receptor for mRNA export [46, 47].

A large number of DEAD-box RNA helicases are also implicated in ribosome biogenesis. In yeast, more than 200 protein cofactors and 75 snoRNAs are involved in ribosome biosynthesis within which 15

are DEAD-box RNA helicases [48]. In humans, three out of four rRNAs, 28S, 18S, 5.8S rRNAs, are transcribed by RNA Polymerase I, whereas the 5S rRNA is transcribed by RNA Polymerase III. Several RNA helicases have been implicated in rRNA synthesis in mammals, however not all of them are well characterized. Nevertheless, a number of RNA helicases in mammals have homologs in yeast RNA helicases and are thought to have similar functions in mammals which has been experimentally supported in some cases. Nearly 22 DEAD-box RNA helicases are said to be involved in human ribosome biogenesis [48, 49].

Translation

DDX2 (eIF4A), the smallest member of the DEAD-box family plays a critical role in cap-dependent translation initiation in eukaryotes. Most eukaryotic translation occurs in a cap-dependent manner and involves eIF4F complex consisting of three subunits including eIF4A. eIF4A possesses RNA helicase activity and unwinds secondary structures present in the 5' UTR region of the mRNA and facilitates the scanning of 40S ribosomal subunit towards the start codon [50-52]. The detailed role of eIF4A in translation initiation is described in further sections of this thesis. In addition to eIF4A, DDX3X has also been implicated in resolving the highly structured 5'-UTR regions of cellular and viral mRNAs and to facilitate ribosome recruitment [53-57]. It does so by directly interacting with the helix 16 on the 40S ribosomal subunit [48, 58]. DDX19B is essential for recognition of stop codons and for recruitment of eRF3, a eukaryotic polypeptide chain release factor to termination complexes [32].

mRNA decay

DDX6 helps in decapping the 5' end of the mRNA and its degradation by exoribonuclease XRN1 [32, 59, 60]. Non-sense mediated decay (NMD) is a critical mRNA surveillance program triggered by the

presence of a premature termination codon (PTC) 50-55 nucleotides upstream of the exon-junction complex (EJC) and degrades the mRNA in order to prevent the formation of truncated proteins which could otherwise exert dominant negative effects. DDX48 (eIF4A3) is one of the four components of EJC and is involved in NMD-mediated removal of PTCs [48, 61, 62].

Cytoplasmic transport and storage

The transportation and storage of mRNAs in the RNA granules has an influence on mRNA translation and degradation [32, 48]. DDX6, DDX4 and DDX3X are involved in mRNA localization in certain cell types and control the translation of the same [32]. Several other DEAD-box proteins are a component of RNA-transporting granules and play a significant role in localized protein synthesis [32, 63, 64].

The above examples show the diverse roles of DEAD-box RNA helicases at various steps of gene regulation. A significant number of these helicases are implicated in more than one step of gene regulation. However, the exact mechanisms through which they are involved in these gene regulation processes is not fully understood and needs to be experimentally validated.

1.3 Protein Synthesis

Translation is a process whereby a messenger RNA (mRNA) is translated into a sequence of amino acids by ribosomes to produce a protein. It is the most energy-intensive process in cells as it consumes up to 20% of cellular ATP [65, 66]. It plays a significant role in gene expression and hence is tightly regulated. The process of protein synthesis is divided into four distinct phases: initiation, elongation, termination and ribosome recycling [50]. Each of these steps is under extensive regulation and any mis-regulation in these

steps can lead to diseased states. For instance, there is a dramatic increase in protein synthesis in tumor cells to fulfil their requirements for growth and proliferation [67]. Moreover, many viruses are dependent on the translation machinery in host cells to facilitate their own replication [68]. Although all the steps are highly regulated, most of the translational control occurs at the initiation step [69]. Translation initiation is an intricate and rate-limiting step in eukaryotic translation which ends with the ribosome recruitment phase and positioning of an elongation competent 80S ribosome at the start codon of the mRNA [70]. It is a complex process that involves coordination of several initiation factors. Eukaryotic protein synthesis can occur by two mechanisms: cap-dependent fashion and cap-independent fashion, with the former being more typical in cells. The text discussed herein will strictly focus on cap-dependent eukaryotic translation initiation.

1.3.1 Cap-dependent translation initiation

Cap-dependent translation in eukaryotes commences with the recognition of 7-methylguanosine (m^7 -Gppp) cap at the 5' end of the mRNA by eIF4E, a small cap-binding subunit of the heterotrimeric eIF4F complex. Apart from eIF4E, eIF4F complex comprises of eIF4A, a DEAD-box RNA helicase and eIF4G, a scaffolding protein. After cap recognition, eIF4G interacts with the RNA via its RNA binding domain and stabilizes the eIF4F complex at the 5' UTR of the mRNA. Thereafter, there is recruitment of ternary complex (TC) that consists of eIF2, methionyl-initiator transfer RNA (Met-tRNA_i) and GTP. This ternary complex is recruited to 40S ribosomal subunit along with other initiation factors including eIF1, eIF1A, eIF3, eIF5 giving rise to a 43S pre-initiation complex (43S PIC). eIF4A remodels the secondary structure in mRNA 5' UTR regions in an ATP-dependent manner along with the help of RNA chaperones (eIF4H and eIF4B). The 43S PIC then binds this region and hydrolyzes GTP. Next, 43S PIC scans the 5' leader region in search of an initiation codon where it releases eIF1 and eIF2-GDP, eIF5 and Pi. Later,

eIF5B-GTP complex binds and recruits the 60S ribosomal subunit. GTP is hydrolyzed and eIF5-GDP complex is released along with eIF4A and Pi resulting in the formation of an elongation-competent 80S ribosome (Figure 3) [50, 71]. The PABP that is bound to poly(A) tail, interacts with eIF4G to form an mRNA closed loop and synergistically stimulates translation along with the eIF4F complex [50, 72, 73].

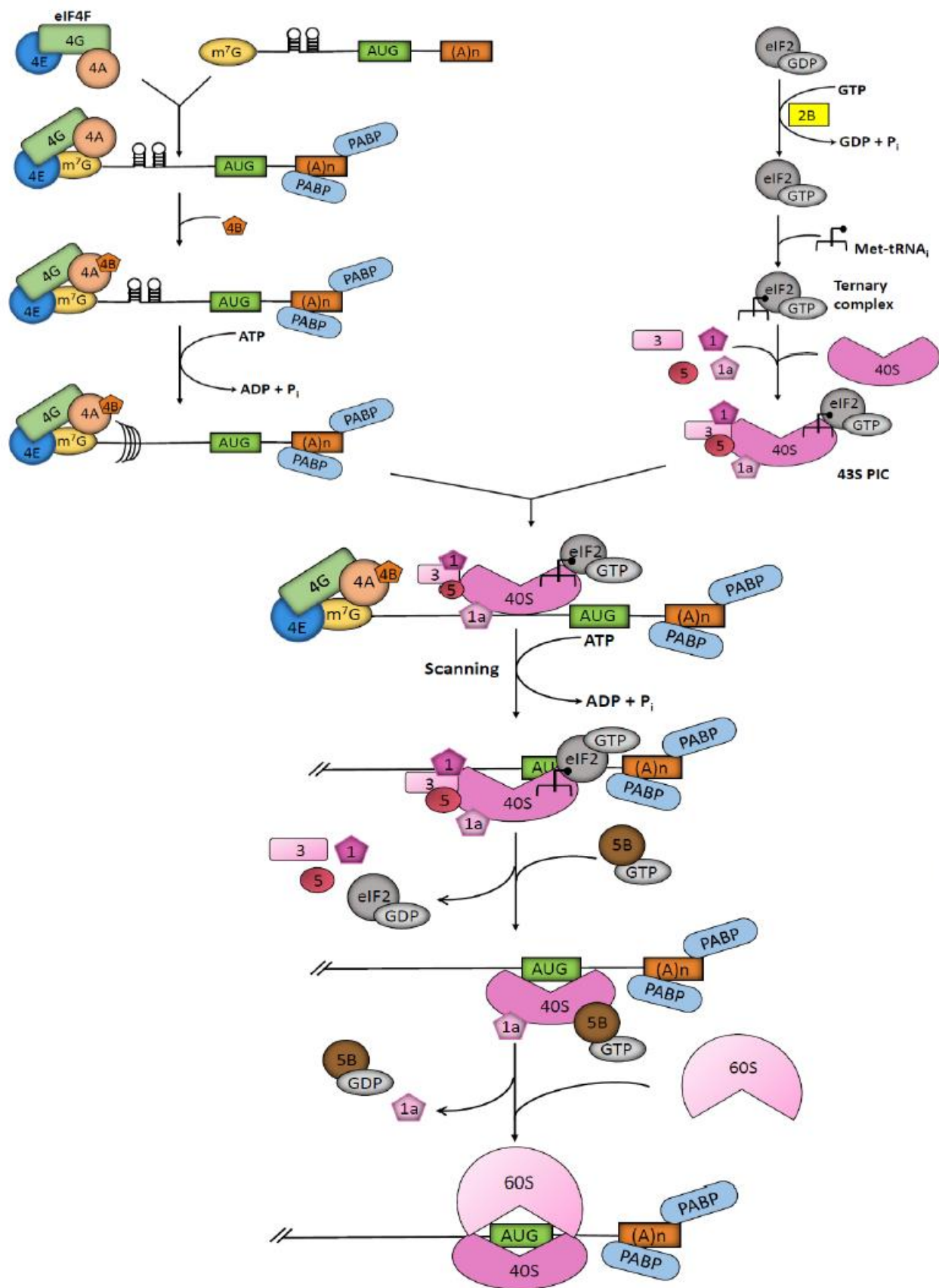


Figure 3: Overview of cap-dependent eukaryotic translation initiation. *Please note that circularization of mRNA is not shown to simplify the illustration.* First, eIF4E binds to the m⁷-Gppp cap structure at the 5' end of the mRNA. eIF4G interacts with the RNA and stabilizes the eIF4F complex at 5' end. A ternary complex consisting of eIF2, Met-tRNA_i and GTP is recruited to 40S ribosomal subunit along with other initiation factors resulting in formation of a 43S PIC. eIF4A in conjunction with accessory factors eIF4B and eIF4H, resolves the secondary structures present in the 5' UTR region of the mRNA in the presence of ATP. 43S PIC binds to this region and scans the mRNA in 5' → 3' direction until it finds an initiation codon (AUG). A 60S ribosomal subunit is recruited and binds to 40S ribosomal subunit with the help of eIF5 at the expense of GTP hydrolysis resulting in the formation of 80S ribosome.

1.3.2 The eIF4F complex

eIF4F plays an indispensable role in ribosome recruitment process of translation initiation. It is a heterotrimeric complex comprising of three subunits: eIF4E, eIF4G, and eIF4A.

eIF4E

eIF4E is a cap-binding protein that plays an important role in controlling gene expression during translation [74]. The mammalian genome encodes three paralogs of eIF4E namely, eIF4E1 (will be referred as eIF4E in this text), 4EHP (eIF4E2) and eIF4E3. 4EHP and eIF4E3 share 30% and 29% identity with eIF4E respectively [75]. All three paralogs can bind to the cap structure of the mRNA (with eIF4E showing the highest affinity). eIF4E and eIF4E3, but not 4EHP, also interact with eIF4G [50]. eIF4E is the best-characterized cap-binding protein and is involved in translation initiation. It is the least abundant initiation factor and hence renders translation initiation rate-limiting. It binds to the m⁷G of the cap structure through tryptophan residues (W58 and W104) by forming cation- π interactions. eIF4G binds to the dorsal surface of eIF4E and recruits eIF4A to the 5' UTR resulting in increased translation rates [76, 77]. eIF4F levels in cell is regulated by eIF4E binding proteins (4E-BPs) [78]. Under non-phosphorylated conditions, 4E-BPs competitively bind to eIF4E and prevent its binding to eIF4G leading to reduced

mRNA translation. However, PI3K- mediated mTORC1 activation leads to phosphorylation of 4E-BPs causing the release of eIF4E which participates in translation initiation [79, 80]. 4EHP has been implicated in translation suppression of select mRNAs during embryonic development. The role of eIF4E3 in translation is not well characterized [50].

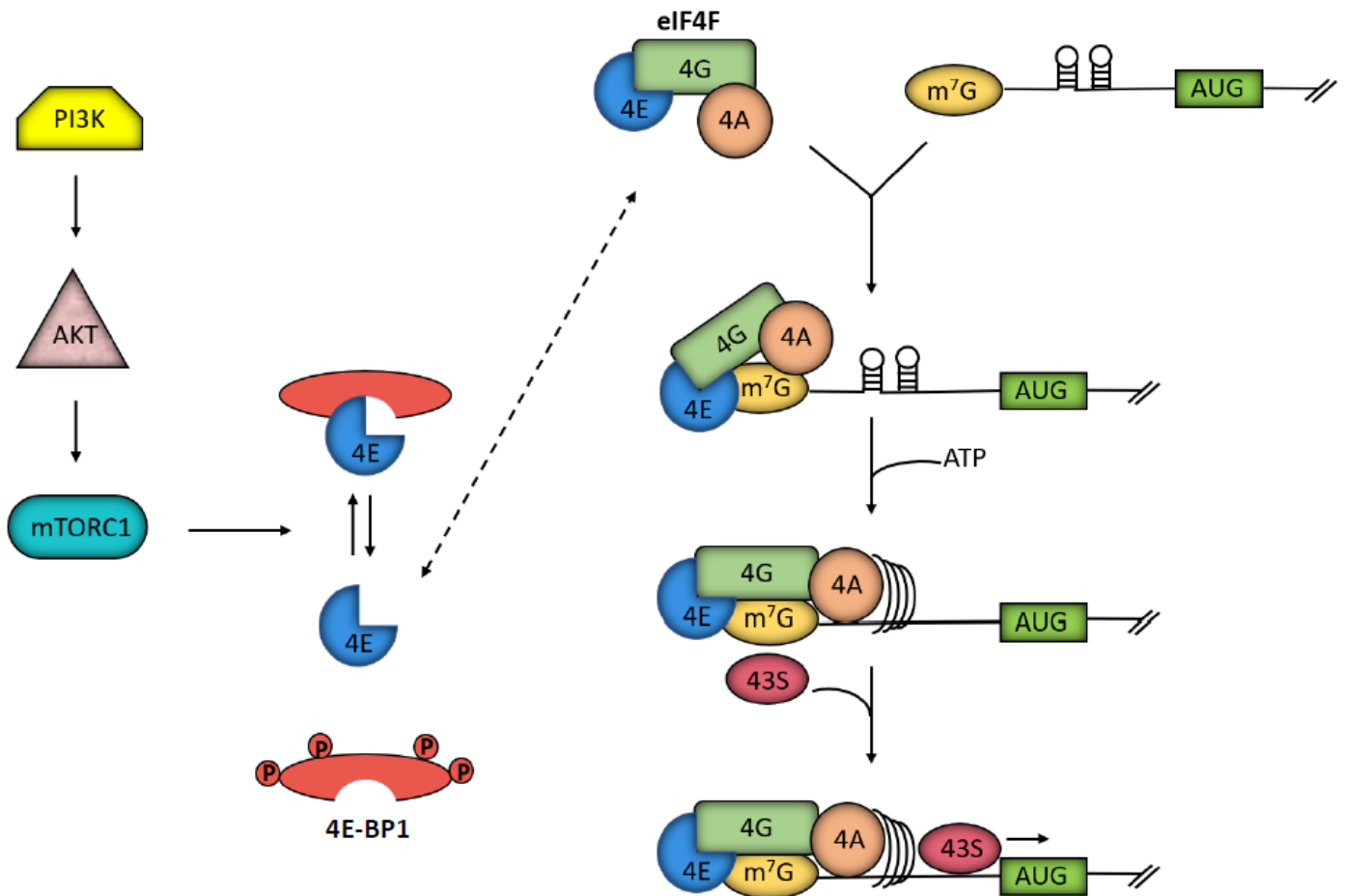


Figure 4: Assembly of eIF4F complex and its role in translation initiation. mTORC1 regulates the eIF4F dependent translation initiation. Binding of eIF4E to 4E-BP1 results in reduced eIF4F levels. 4E-BP1 is a direct substrate for mTORC1 which phosphorylates 4E-BP1 causing its dissociation from eIF4E. This allows eIF4E to join the eIF4F complex. Binding of eIF4F to 5' mRNA cap structure enables eIF4A to resolve secondary structures in an ATP-dependent manner and facilitates ribosome recruitment.

eIF4G

The scaffolding protein eIF4G interacts with eIF4A, eIF4E, eIF3, PABP and mRNA [50]. There are three paralogs in humans: eIF4G1, eIF4G2 and eIF4G3. eIF4G1 and eIF4G3 are 46% similar at the amino acid level and can be segregated into three regions, NTD, middle domain (MIF4G) and CTD [81, 82]. NTD contains binding sites for both eIF4E and PABP and helps in mRNA circularization [83, 84]. Three HEAT domains are present in eIF4G out of which HEAT domain 1 (HEAT-1) is present in the middle region, while HEAT-2 and HEAT-3 are present in the CTD. HEAT domains are required for eIF4A binding. HEAT-1 and HEAT-2 bind to NTD and CTD of eIF4A, where binding with HEAT-1 holds eIF4A into its half-open conformation that triggers its ATPase and RNA binding activity. The interactions between N-terminal eIF4A and C-terminal eIF4G holds eIF4A in its closed conformation [85]. This conformational cycle is essential for ATP-dependent RNA unwinding by eIF4A. [86-88]. As well, MAP-kinase interacting kinase (MNK) 1 and 2 bind to eIF4G at its CTD HEAT domain. MNK1 phosphorylates eIF4E at S209 which increases the translation of select mRNAs [89].

eIF4A

The human genome encodes three paralogs of eIF4A: eIF4A1 (DDX2A), eIF4A2 (DDX2B) and eIF4A3 (DDX48) [90, 91]. eIF4A1 and eIF4A2 share 90% identity at the amino acid level and are involved in translation initiation with the former being more abundant and essential for survival [50]. eIF4A3 is 66% identical at the amino acid level with eIF4A1 and plays a vital role in NMD [92-94]. eIF4A1 is produced during active cell growth while eIF4A2 is overexpressed during growth arrest [50]. Studies have also shown that suppressing eIF4A1 leads to elevation in eIF4A2 levels in cells, however it is not enough to compensate the loss of eIF4A1 in cells resulting in cell death [95-97]. eIF4A unwinds the

secondary structures in mRNA from the 5' to 3' end and this directionality is conferred by the eIF4G RBD [98]. eIF4A1 can unwind around 10-15 nts in length and 10-12 base pairs per molecule of ATP hydrolyzed [50, 98]. It has also been reported that RNA fragments of merely 4 nucleotides are enough to initiate the ATPase activity of eIF4A1 but RNA fragments of 15-20 nts are preferred [99]. eIF4A in the presence of its cofactors eIF4B and eIF4H increases translation initiation as they increase the processivity of eIF4A [98]. eIF4B helps in enhancing the ATPase and helicase activity of eIF4A and also increases the coordination between these two processes. Moreover, it has also been shown to increase the translation of mRNAs with complex structures within the 5' end in an eIF4A independent manner [100]. eIF4H is related to eIF4B and shares 39% amino acid identity with the latter. Both eIF4B and eIF4H bind at the same site on eIF4A and hence only one of them can bind to it at any given time [101]. eIF4A dependency of mRNA translation increases with complexity of mRNA 5' ends. The availability of eIF4A for translation initiation is a subject to regulation by PDCD4. PDCD4 binds to eIF4A and hinders the formation of its active closed conformation by masking the RNA-binding site of eIF4A [102, 103].

1.4 Targeting DEAD-box RNA helicases as therapeutic vulnerabilities in cancer

DEAD-box RNA helicases play a critical role in different cellular processes that are often dysregulated in cancers. Dysregulation in the helicase activity of these proteins can have serious repercussions on normal cellular homeostasis and can lead to tumor development and progression [51, 104, 105]. Several DEAD-box proteins are overexpressed in human cancers [106]. Moreover, they also act as interacting partners with some oncogenic transcripts and lead to tumor progression [107]. There are three biological processes where the role of DEAD-box RNA helicases has been associated with cancer

development: Translation initiation, nonsense mediated decay and ribosome biogenesis [48]. Since ribosome recruitment is the rate limiting step in protein synthesis, there has been much interest in targeting this step in cancer cells. Several mRNAs with higher secondary structures in their 5' UTR show increased dependence on eIF4F complex for their translation. In cancer cells, there are two pathways whose activities are often deregulated and which affect eIF4F's normal activity. PI3K/ Akt/ mTORC1 signaling pathway regulates the assembly of eIF4F complex by phosphorylating 4E-BP1 and increasing eIF4E levels available for eIF4F which in turn increases the translational output [78, 108-110]. In addition to this, PDCD4 that binds to eIF4A and reduces translation is also under the regulation of PI3K/ Akt/ mTORC1 pathway. Stimulating this pathway results in phosphorylation of PDCD4 leading to its degradation, thus increasing eIF4A availability for initiation [111-113]. Hence, eIF4F/ eIF4A serves as an important druggable target for cancer [51, 114]. Besides eIF4A, other helicases like DDX3X, DDX4, DDX19B, DDX41 have also been implicated in translation initiation although, unlike eIF4A1, their exact role is not well characterized. DDX3X in mammals, has been shown to have both stimulatory and inhibitory activity in translation initiation [115]. Recent experimental evidence demonstrates that DDX3X increases the translation of highly structured mRNAs and is also suggested to be overexpressed in breast cancer and viral- associated cancers [116-119]. DDX4 is required for proliferation and differentiation of germ cells in mouse but its mechanism of action is yet to be explored [115]. Nonsense-mediated decay of the mRNA (that involves DDX48) is a process where transcripts with nonsense mutations are subjected to degradation. However, failure to do so in specific tumor suppressor genes may lead to progression of prostate cancer cells and development of other tumors [120]. Increased ribosomal RNA synthesis due to elevated MYC levels is also correlated with uncontrolled and abnormal cell growth in cancers. In cellula, DDX5 in absence of tumor suppressor ARF, increases the translational output and shows growth-stimulatory functions in ribosome biogenesis [121]. Thus, targeting DDX5 and other DEAD-box proteins

that are implicated in elevated rRNA production leading to tumorigenesis may serve as potential anti-cancer targets.

1.5 Small molecule inhibitors of DEAD-box RNA helicases

1.5.1 DDX2 (eIF4A)

Three natural products (Hippuristanol, Pateamine A, Rocaglates) demonstrating inhibitory activity towards eIF4A1/eIF4A2 were uncovered from a high-throughput screen of >200,000 compounds performed to identify modifiers of translation [122].

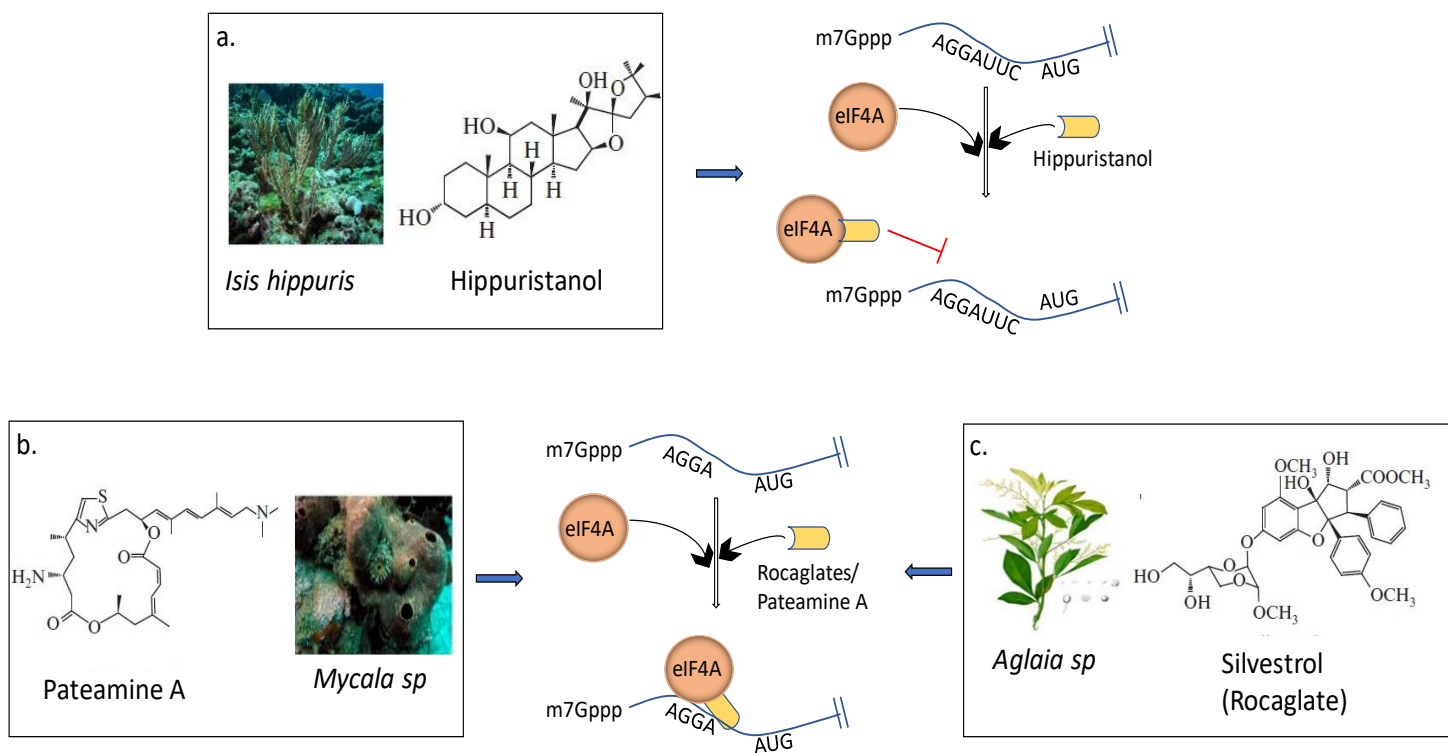


Figure 5: Small molecule inhibitors of eIF4A. (a) Hippuristanol inhibits the binding of eIF4A onto the RNA and inhibits translation initiation. (b) Pateamine A clamps eIF4A onto RNA and stabilizes this complex to prevent 43S PIC scanning of the 5' leader region of the mRNA. (c) Rocaglates clamp eIF4A onto purine rich regions of mRNA and stabilize the eIF4A1:RNA complex. *The pictures of plants and marine sponges are taken from (a) Ref. [123], (b) Ref. [124], (c)Ref. [125].*

Hippuristanol

Hippuristanol is a polyoxygenated steroid obtained from the soft coral, *Isis hippuris* [126] (Figure 5a). It binds to the C-terminal domain of eIF4A and locks it in its closed conformation such that it interferes with the RNA binding site and inhibits the RNA-dependent ATPase activity of eIF4A1 [52, 127-129]. It prevents the binding of both free eIF4A and eIF4F bound eIF4A onto the RNA [129]. NMR data suggests that hippuristanol interacts with the amino acid residues from and adjacent to motifs V and

VI that are implicated in RNA binding and coordinating RNA and ATP interdomain contacts respectively [127]. The adjacent amino acid residues are not conserved through the mammalian DEAD-box RNA family rendering this compound selective to eIF4A1/eIF4A2. Since it doesn't interact with the ATP binding sites largely lying in the N-terminal domain, hippuristanol doesn't interfere with the ATP binding activity by eIF4A1 [127, 130]. In the case of eIF4A3, it has been shown that hippuristanol can inhibit the ATPase activity of eIF4A3 in vitro, although at a relatively lower potency than eIF4A1. This result was attributed to the less conserved amino acid residues between eIF4A1 and eIF4A3 at hippuristanol binding site [127]. Further, it has been found that increases in length of mRNA 5' leader regions, as well as increases in GC and C content, enhances the Hipp-responsiveness in mRNAs [131]. Hippuristanol exhibits potent activity against lymphocytic leukemia P-388 tumors in mice and against primary effusion lymphoma [129, 132, 133]. In addition to this, hippuristanol has also been shown to resensitize tumor cells to doxorubicin in an E μ -Myc mouse lymphoma model [134]. Furthermore, it shows synergistic effects with ABT-737, a Bcl2 inhibitor and dexamethasone against mouse lymphoma cells and multiple myeloma cells respectively [134, 135].

Pateamine A

Pateamine A is a marine product obtained from *Mycale* species (Figure 5b) [136]. Unlike Hippuristanol that inhibits the RNA binding to eIF4A1, Pateamine A stimulates the eIF4A:RNA binding in a sequence independent manner resulting in reduced availability of eIF4A for eIF4F complex. This in turn inhibits cap-dependent translation initiation. Pat A does not clamp eIF4F bound eIF4A onto the RNA, but rather affects only free (unbound) eIF4A, which suggests that in its eIF4F bound state, the binding site of eIF4A and Pat A is obstructed [137-139]. It has been previously reported that Pat A possesses anti-neoplastic activity against wide range of cultured human cancer lines. DMDA-Pat A, a synthetic analogue

of Pat A is less cytotoxic than the latter and has similar activity profile on eIF4A1. Moreover, it is well tolerated and inhibits tumor growth in mouse melanoma xenograft models [140].

Rocaglates

Rocaglates were first isolated in the *Aglaia* genus of the angiosperm Mahogany (Meliaceae) family (Figure 5c). They share a common cyclopenta[b]benzofuran skeleton (Figure 6b). Rocaglamide A (Roc A) was the first rocaglate isolated from this source that exhibited anti-leukemic activity in mice [141]. Ever since, several rocaglates have been synthesized and tested for evaluating their anti-neoplastic activity. Silvestrol, a naturally derived member of this family is one of the best studied rocaglates that affects translation initiation by stabilizing eIF4A1 onto purine-rich mRNA regions [91, 142, 143]. The effect of rocaglates on protein synthesis have been extensively studied. mRNAs with complex 5' UTR structures show higher sensitivity towards inhibition by rocaglates according to a study conducted by Rubio *et al* (2014) [144]. However, later it was reported that presence of complex structures in the 5' leader region of the mRNA is not the only determining factor of Roc A's sensitivity and that polypurine content is also important. The detailed mechanism by which rocaglates exert their inhibitory effect on global translation was reported by Chu *et al.* (2020) [145]. Rocaglates clamp eIF4A onto purine bases in the 5' UTR and inhibit the scanning of the 43S PIC towards the start codon. Rocaglates can also trap the eIF4F complex at 5' cap structure and directly inhibit the translation of target mRNAs by blocking the 43S PIC recruitment to the same. Moreover, by increasing the retention time of the eIF4F complex at cap structure, they reduce the levels of free eIF4F and inhibit the translation of mRNAs that are not directly targeted by eIF4F [145]. Earlier studies in yeast eIF4A1 showed that P147 (P159 in heIF4A1), F151 (F163 in heIF4A1), Q183 (Q195 in heIF4A1) and I187 (I199 in heIF4A1) are critical for rocaglate binding. Later, it was further validated that eIF4A1 target engagement by rocaglates is essential for its anti-

neoplastic activity by incorporating the F163L mutation into the murine eIF4A1 cDNA (a mutation that renders eIF4A1 resistant to rocaglates) [146]. The structural basis for these findings were further supported by the crystal structure of eIF4A1·AMPPNP·RocA·(AG)₅ RNA generated by Iwasaki *et al.* (Figure 6a) [147]. The crystal structure revealed that Roc A fits in the bimolecular cavity formed by NTD of eIF4A1 and two sharply bent purine bases A7 and G8. Out of the three phenyl rings in Roc A, ring A is stacked with adenine base of A7 via π - π interaction and ring B with guanine base of G8. Through structural modeling it was found that replacing A7 with a pyrimidine base hampers the stacking of ring A with the pyrimidine base given its smaller size. The PIEDA analysis indicates that hydrogen bond formed between 8b-OH and N7 of G8 dictates the purine selectivity of Roc A. Replacing G8 with a pyrimidine impedes the formation of hydrogen bond and weakens the contact between the RNA and Roc A suggesting that only purine bases are capable to form a bimolecular cavity that can accommodate Roc A. Hence, modifying rocaglates at ring A, ring B and/or 8b-OH may change the shape of the bimolecular cavity and may offer varying base selectivity [147]. Ring C of Roc A is wedged between phenylalanine at position 163 and glutamine at position 195 of eIF4A1 (Figure 6c). The carbonyl group in 2-N,N-dimethyl-carboxamide participates in hydrogen bonding with NH₂ group of Gln195 in eIF4A1 (Figure 6c). Besides, Gly160, Pro159, Ile199 and Asp198 surround the ring C (Figure 6a) [147]. The structural insights into rocaglates and their target engagement with eIF4A1 have been crucial in modifying these compounds to optimize their binding and design better compounds with higher potency and efficacy. In the recent years, the Porco lab has synthesized several rocaglate congeners and has produced amidino rocaglates, a novel series of rocaglates. They are the most potent compounds found against eIF4A1 to date and possess potent cytotoxic effects and translation inhibition activity both in vitro and in cellula [148]. Rocaglates have shown preclinical efficacy as chemotherapeutic agents in various cell lines and mouse models. Rocaglates have also shown to exhibit synergistic effects with dexamethasone in MM cells and with DNA damaging

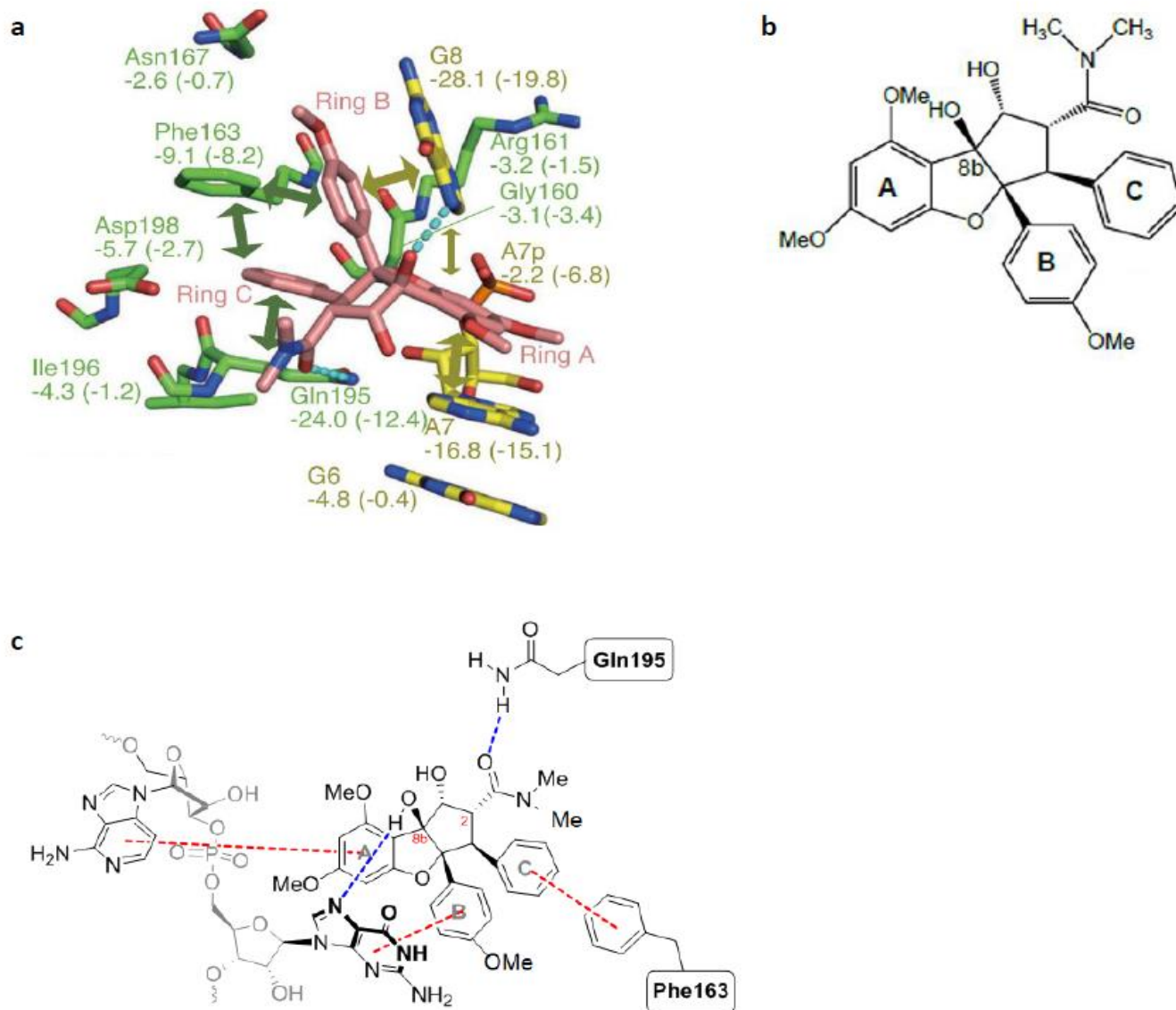


Figure 6: Structural basis of rocaglate binding to eIF4A1. (a) Schematic diagram showing RocA (red)-eIF4A1 (green) interactions. Dark green double-headed arrows show ring C of RocA interacting with phenylalanine 163 and glutamine 195 of eIF4A1; RocA-RNA (yellow) interactions, dark yellow double-headed arrows show ring A of RocA stacked with adenine base of A7 and ring B of RocA stacked with guanine base of G8; hydrogen bonds with RocA are shown in dashed light blue lines. (b) Structure of Rocaglamide A. (c) Schematic diagram showing interaction of RocA with eIF4A1 at F163 and Q195 of eIF4A1. The bonds shown in red represent π - π interaction. The bonds shown in blue represent hydrogen bonding. Figure 5(a) taken from Ref. [147]. Figure 5(c) made by Dr. Lauren Brown, Boston University.

agents in various cell lines [134, 142, 149]. Altogether, rocaglates present as attractive candidates to target protein synthesis in the cancer setting.

1.5.2 DDX3X

DDX3X has been implicated in transcription, pre-mRNA splicing, and translation. Mutations in DDX3X have been indicated in various cancers including, chronic myeloid leukemia [150], head and neck cancer [151], melanomas [152] and many more [47]. Moreover, DDX3X is also implicated in HIV-1 and HCV replication [153]. Hence, there has been an emerging interest in targeting this helicase and a few small molecules have been developed against the same. Rhodamine analogs and ring-expanding nucleosides (RENs) inhibit the ATPase activity of DDX3X and the latter have shown their anticancer activity in lung cancer, Ewing sarcoma and various other cancers [48, 154-157]. Other congeners of the REN class of compounds are being developed to optimize their activity against DDX3X. Ketorolac salt has also shown to inhibit ATPase activity of DDX3X and is effective against oral cancer in *in vivo* settings [158]. Moreover, Iwasaki and group showed that Roc A can target DDX3X *in vitro* although, at lower potency than eIF4A1 [159].

1.5.3 DDX5

DDX5 is involved in activation of Wnt target genes like cyclin D1 and Myc. Hence, it serves as a potential antineoplastic target in cancer since Myc is known to be overexpressed in several cancers [160]. RX-5902 is a compound that binds to phosphorylated DDX5 and inhibits its β -catenin dependent ATPase activity [48, 161]. This candidate is under clinical trials and has been tested for the treatment of breast cancer where it arrests the cell cycle at G2/M phase leading to cell death [162, 163].

1.5.4 DDX48

DDX48 is a central component of EJC and plays a critical role in NMD. In various cancers, NMD contributes to complete inactivation of tumor-suppressor genes and thereby promotes tumor growth [164]. Hence, developing small molecules against DDX48 to achieve NMD inhibition to treat tumors has gained a lot of interest [164, 165]. This desire has led to identification of 1,4-diacylpiperazine series of compounds (compounds 52a and 1q) [165]. These compounds bind to the CTD of DDX48 and allosterically inhibit its ATPase activity [62]. It was further found through a CRISPR-based variomics screen that NMD inhibition by these molecules is linked to DDX48 target engagement [165]. Moreover, compound 1q has been reported to retard the tumor cell growth in HCT-116 colorectal cancer cells [165, 166].

1.6 Overview and rationale for the thesis

The DEAD-box protein family is a family of putative RNA helicases that are said to be involved in all the stages of the RNA life cycle. Disruption of their function is implicated in various diseases including but not limited to cancers. Hence, targeting these helicases is a promising therapeutic strategy to overcome these conditions. Rocaglates clamp eIF4A (DDX2) onto the purine rich regions of RNA and stabilize this complex which in turn impedes the 43S PIC scanning and halts the translation at this step. Rocaglates exert their effects by interacting with phenylalanine at position 163 and glutamine at position 195 of eIF4A1. Since the interaction sites for rocaglates have been well established with eIF4A1 [147], and that DEAD-box RNA helicases have a structurally highly conserved core, we checked the amino acid diversity of these residues in other DEAD-box family members (Table 1). The presence of different amino acids at these key interacting positions offers an opportunity to target these helicases. Our collaborators had designed a rocaglate library by modifying certain functional groups which we tested to find the ones that are selective towards a particular DDX helicase. For instance, DDX20, DDX21 and DDX50 have a lysine at the position corresponding to eIF4A1 F163. Hence, if the C ring in Roc A is substituted with an electron donating group, then it could potentially induce cation- π interactions with lysine in these helicases (Figure 7). As a preliminary screening for compounds, we generated eIF4A1 mutants with mutations at F163 or Q195 or both F163/Q195 to mimic the residues present in other DEAD-box helicases at these positions. We tested this rocaglate library with mutant eIF4A1 proteins to identify rocaglates that exert specificity towards a particular eIF4A1 mutant. Should we obtain any compound specific towards a mutant, it would be further optimized for binding with the corresponding DEAD-box helicase. The findings obtained from the preliminary screening of the compounds have been described in this thesis. We aim to design novel inhibitors against DEAD-box RNA helicases to unravel their functions in cellular

processes and that might function as therapeutic agents against various diseased states caused by them, especially cancer.

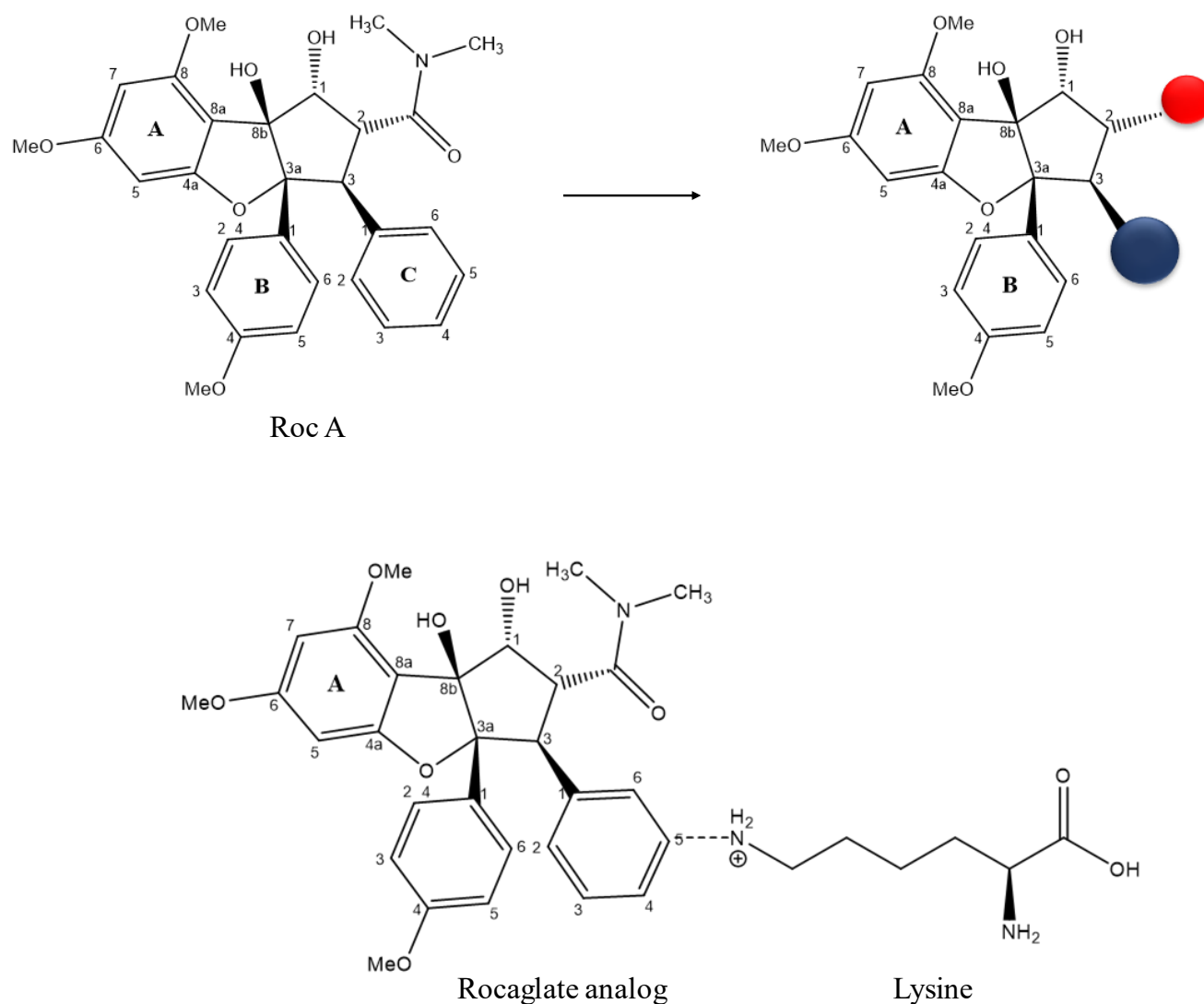


Figure 7: Strategy to target a specific DEAD-box RNA helicase. Modifying the C-ring to an electron rich ring induces cation- π interaction with lysine in F163K.

2. MATERIALS AND METHODS

2.1 General materials:

5'-FAM-labelled poly (AG)₈ RNA was obtained from Integrated DNA Technologies (IDT). AMP-PNP was procured from Jena Bioscience (Cat#: NU-407-50).

2.2 Compounds:

Rocaglate derivatives were provided by Dr. Lauren Brown and Dr. John Porco from their BU-CMD collection at Boston. The compounds were resuspended in 100% DMSO to a final concentration of 10 mM and stored at -20 °C.

2.3 Construction of expression vectors:

pET-15b-His₆-eIF4A1 (WT or mutant) plasmid was used to express the recombinant proteins. All recombinant DNA constructs for protein expression were obtained from Sai Kiran Naineni (a graduate student in lab) except pET-15b-His₆-eIF4A1 (F163I, Q195D, Q195E). To generate eIF4A1 mutants with desired amino acid substitution, G blocks with desired mutations were procured from IDT. G blocks were digested using KpnI and NsiI restriction enzymes and subcloned into pET-15b-His₆-eIF4A1. Clones were sequence verified by Sanger sequencing.

2.4 Expression and purification of recombinant proteins:

The recombinant DNA plasmids were transformed into BL21 (DE3) pLysS competent cells and plated on LB Ampicillin plates (100 µg/mL). Single colonies were picked and inoculated in 50 mL LB media

supplemented with 100 µg/mL ampicillin and 34 µg/mL chloramphenicol overnight at 37°C to grow a starter culture. Next day, the culture was diluted 1:20 and grown at 37°C till the O.D₆₀₀ reached between 0.6- 0.8. Expression of the protein was induced with 0.5 mM or 1 mM IPTG at 16°C overnight (approximately 16 hours). Cells were harvested at ~4000 xg and were resuspended in sonication buffer (20 mM Tris pH 7.5, 10% glycerol, 0.1 mM EDTA, 200 mM KCl, 0.1% Triton X-100 and 3.4 mM β-mercaptoethanol) followed by sonication. The cell lysate was cleared by centrifuging the cells at 10,000 rpm for 20 minutes at 4°C. The supernatant was loaded on pre-equilibrated Ni-NTA agarose beads for 1 hour at 4°C on a rotating platform. The supernatant was allowed to pass through the beads and the beads were washed twice with 10 mL wash buffer 1 (20 mM Tris pH 7.5, 10% glycerol, 0.1 mM EDTA, 800 mM KCl, 20 mM imidazole) followed by a wash with 10 mL wash buffer 2 (wash buffer 1 containing 300 mM imidazole). The protein was eluted in 3 mL elution buffer (20 mM Tris pH 7.5, 10% glycerol, 0.1 mM EDTA, 300 mM KCl, 2mM DTT and 200 mM imidazole). The protein was dialysed at 4°C overnight in a dialysis buffer (20 mM Tris pH 7.5, 10% glycerol, 0.1 mM EDTA, 300 mM KCl, 2mM DTT). Some protein samples were further purified using a Q-Sepharose fast flow column and were eluted using 100-500 mM KCl gradient in 20 mM Tris pH 7.5, 10% glycerol, 0.1 mM EDTA. 500 uL fractions were collected and subjected to SDS-PAGE electrophoresis followed by Coomassie blue staining to assess their purity. The high purity and high yield fractions were pooled and dialyzed in 20 mM Tris pH 7.5, 10% glycerol, 0.1 mM EDTA and 2 mM DTT.

2.5 ATPase assay:

ATPase assay was performed as previously described by Lorsch and Herschlag [167]. Briefly, 2 µM protein was incubated with 1 mCi [γ ³²P]-ATP (3000 Ci/mmol) in the presence or absence of 2.5 µM poly (U) RNA in a buffer containing 2.5 mM MgCl₂, 1 mM DTT, 1% glycerol, 20 mM MES-KOH [pH 6.0], 10 mM

KOAc. Reactions were incubated at 25°C for 30 minutes and 1/10th of the sample was collected and quenched with EDTA at a final concentration of 15 mM at different intervals (t= 0, 2, 5, 10, 20, 30 min). The quenched reactions were resolved on PEI cellulose TLC plates in a mobile phase containing 1 M LiCl and 0.3 M NaH₂PO₄. The extent of ATP hydrolysis was quantified by cutting the separated [γ ³²P]-ATP and Pi regions and were used for measuring the scintillation counts. The quantified ATP hydrolysis was plotted against indicated time points using GraphPad Prism (V 8.4.0).

2.6 Fluorescence polarization assay:

FP assays were performed as previously described by Chu et al., [145]. In essence, 1.5 μ M eIF4A1 (WT or mutant) was incubated with 10 nM FAM-labelled poly (AG)₈ RNA and 1 mM AMP-PNP either in the presence or absence of 10 μ M compound in a buffer containing 14.4 mM HEPES-NaOH [pH 8], 108 mM NaCl, 1mM MgCl₂, 14.4% glycerol, 0.1% DMSO, 2mM DTT in black, F-bottom 384 well polystyrene cell culture microplates (Ref 781086). The reactions were incubated for ~30 minutes at 25°C and the polarization values were measured on a Pherastar FS microplate reader (BMG Labtech).

3. RESULTS

3.1 Qualitative assessment of engineered recombinant proteins.

Rocaglates interact with F163 and Q195 of eIF4A1. Taking the advantage of conserved helicase core in DEAD-box helicases, we looked at the diversity of amino acid residues at these positions in other helicases. We aligned the respective DEAD-box protein sequences with eIF4A1 using NCBI protein BLAST tool. Table 1 shows different residues that are present in these helicases at the key rocaglate interacting positions of eIF4A1. Based on this, we engineered different eIF4A1 plasmids with mutations at F163, Q195 or F163/Q195 and replaced these residues with the ones found in the respective DDX helicase. We did not focus on designing F163A mutation in eIF4A1 (corresponds to DDX49) since the hydrophobicity of alanine (A) is very low and it can only induce weak van der Waal's interaction with the aromatic C ring of rocaglates. In addition to eIF4A1 mutants corresponding to human DDX proteins, we engineered F163Y and F163Q mutations present in *Plasmodium* eIF4A [168] and Microsporidia eIF4A respectively. In addition to these, we incorporated D198R and D198K mutations in eIF4A1. D198 mutants were designed keeping in mind that D198 residue lies near the rocaglate binding site (Figure 6a) [147]. Substituting the aspartic acid residue with either arginine (R) or lysine (K) could induce electrostatic interactions with the C ring of rocaglates. Moreover, these mutants were of interest as DDX3X has an arginine at the corresponding position, whereas DDX5 and DDX17 contain a lysine at the same position (eIF4A1 numbering). Hence, we designed these eIF4A1 mutants for further experiments. These plasmids were expressed in bacterial cells and proteins were purified as described earlier (Figure 8a, b). The quality of the purified proteins was analyzed by Coomassie staining. The size of the purified proteins observed

on the gel was ~48 kDa which was consistent with the calculated molecular weight of His₆-eIF4A1/recombinant eIF4A1 (Figure 8c). It is noteworthy that although eIF4A1 mutants other than the ones corresponding to human DDX helicases were also purified, the work described in further sections of the thesis strictly focuses on human DDX helicases.

Amino acids corresponding to position 163 of eIF4A1

	F	N	W	S	K	L	I	V	A	M	D	E	Properties
Amino acids corresponding to position 195 of eIF4A1	Q	eIF4A1 eIF4A2 DDX48	DDX43 DDX53			DDX20 DDX21 DDX50	DDX9A DDX19 DDX25 DDX59	DDX5 DDX17 DDX27 DDX46 DDX52	DDX3X DDX3Y DDX54				Amide- π bonding, H- bonding
	D					DDX39	DDX23	DDX31	DDX49	DDX41			Anionic bonding
	E			DDX24		DDX18 DDX56	DDX47			DDX4			
	L			DDX28									
	S											DDX55	H- bonding
	I						DDX6						
	F		DDX11					DDX60				DDX1	π -bonding
	T						DDX10						H- bonding
	W				DDX58								π -bonding
	Properties	Moderately sized, flat π -bonding H- bonding			Cation- π	Flexible, Cation- π	Bulky, aliphatic, Van der Waals (VDW) only			Small, VDW only	π - bonding	Moderate, Anionic bonding	

Table 1: Amino acid diversity in mammalian DEAD-box helicases corresponding to position 163 and 195 of eIF4A1 and the properties of these residues.

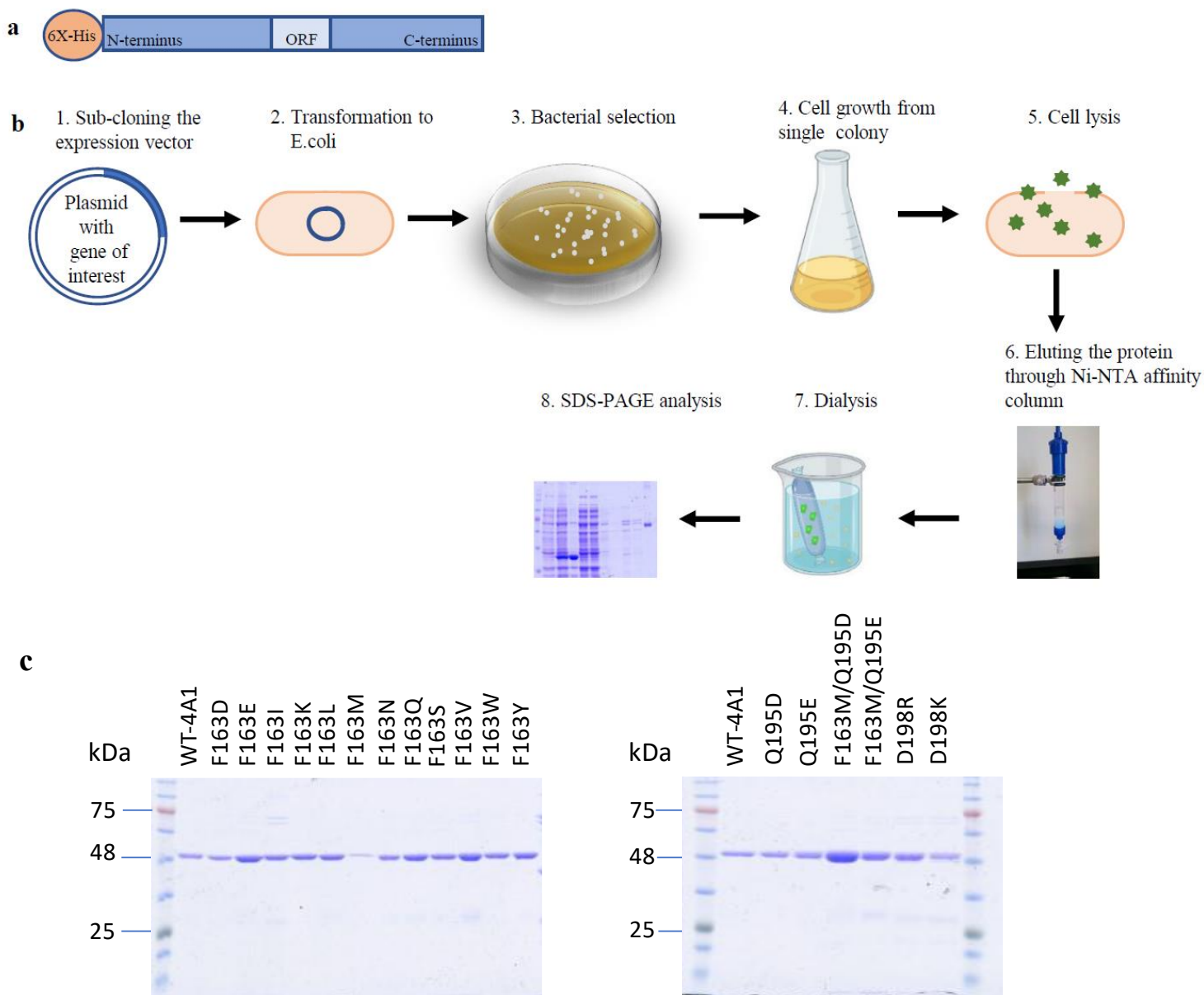


Figure 8: Recombinant protein engineering. (a) Schematic showing His₆-eIF4A1 recombinant protein. (b) Schematic diagram depicting the process of expressing and purifying the recombinant proteins. (c) Coomassie blue staining of SDS-PAGE showing purified recombinant proteins used for further experiments.

3.2 Functional analysis of the wild-type and recombinant eIF4A1 proteins.

To document the effect of these mutations on functionality of these proteins we performed an RNA-dependent ATPase assay. It is well attested that DEAD-box proteins exhibit RNA-stimulated ATPase, RNA helicase activity, and ATP-dependent RNA binding [169, 170]. Hence, following the purification of recombinant proteins, we checked if mutants were functionally active. The time course ATP hydrolysis activity of both WT and mutant eIF4A1 proteins was monitored using 2 μ M protein with γ -³²P-ATP in the presence of poly (U) RNA, and the magnitude of ATP hydrolysis was determined. The ATPase activity of these proteins was also monitored in the absence of RNA after 30 minutes of incubation as a control. The reason why we chose poly (U) RNA is because previous investigations have demonstrated that poly (A) and poly (U) RNA sequences are more potent in stimulating the ATPase activity of eIF4A1, compared to poly(C), poly(I), poly(G), globin mRNA, tRNA or poly(A)·poly(U) substrates [171]. In addition to this, earlier studies have shown strong ATPase activity of eIF4A1 when poly (U) RNA is used as activator [172]. The data plots (Figure 10) represent one phase association fit describing the pseudo-first order association kinetics of the interaction between proteins and γ -³²P-ATP.

We observed that all the protein preparations showed robust ATPase activity in the presence of poly (U) RNA (Figure 9, 10). F163K, D198R and D198K showed higher ATPase activity than WT-eIF4A1 followed by F163M. F163I, F163L, F163W and F163M/Q195D showed ATPase activity but not as strong as WT-eIF4A1. F163D, F163S, Q195D and Q195E exhibited lowest RNA-stimulated ATPase activity. Surprisingly, we observed that all the proteins except F163M were also able to hydrolyze ATP to different extents in the absence of RNA. The reason why these mutants show different ATPase activities is not completely understood but could be the change in ATP binding pocket that might be caused by the presence of different amino acids at F163 and/or Q195 of eIF4A1. F163 and Q195 of eIF4A1 are present

in the DEAD-motif (i.e., motif II) of the helicase core (Figure 1b), a domain which is involved in ATP binding and hydrolysis.

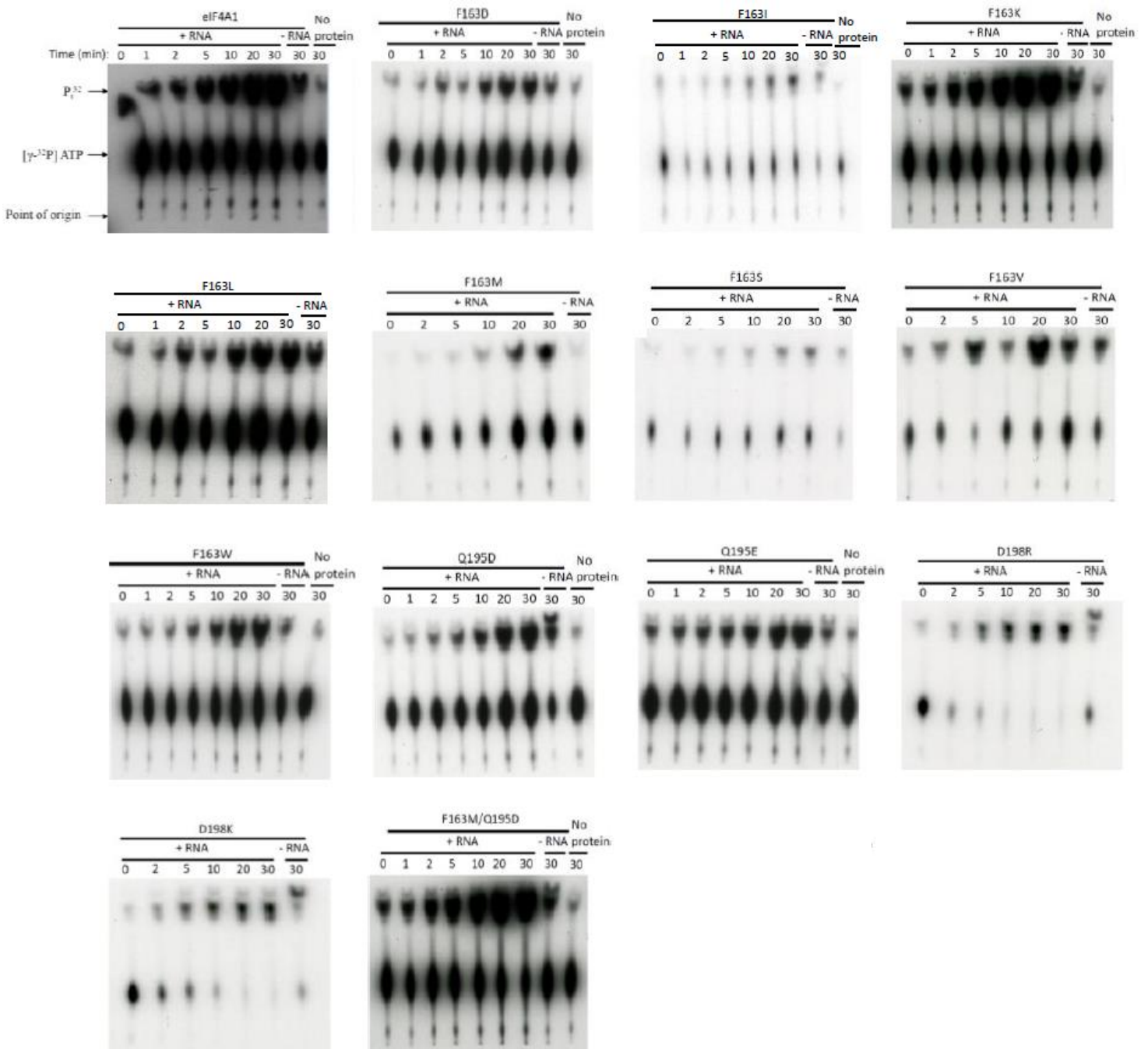


Figure 9: Assessment of ATP hydrolysis by purified proteins via Thin Layer Chromatography (TLC). ATPase activity was evaluated by incubating $2\ \mu\text{M}$ of protein with $1\ \mu\text{M}$, $10\ \text{Ci}/\text{mmol}\ \gamma\text{-}^{32}\text{P}\text{-ATP}$

either in the presence or absence of 2.5 μM poly (U) RNA at 25 $^{\circ}\text{C}$. Reaction sample (2 μL) was aliquoted and sequestered into 15 mM EDTA at indicated time points. The hydrolyzed inorganic phosphate was separated from $\gamma\text{-}^{32}\text{P}\text{-ATP}$ by TLC which were later exposed to an X-ray film.

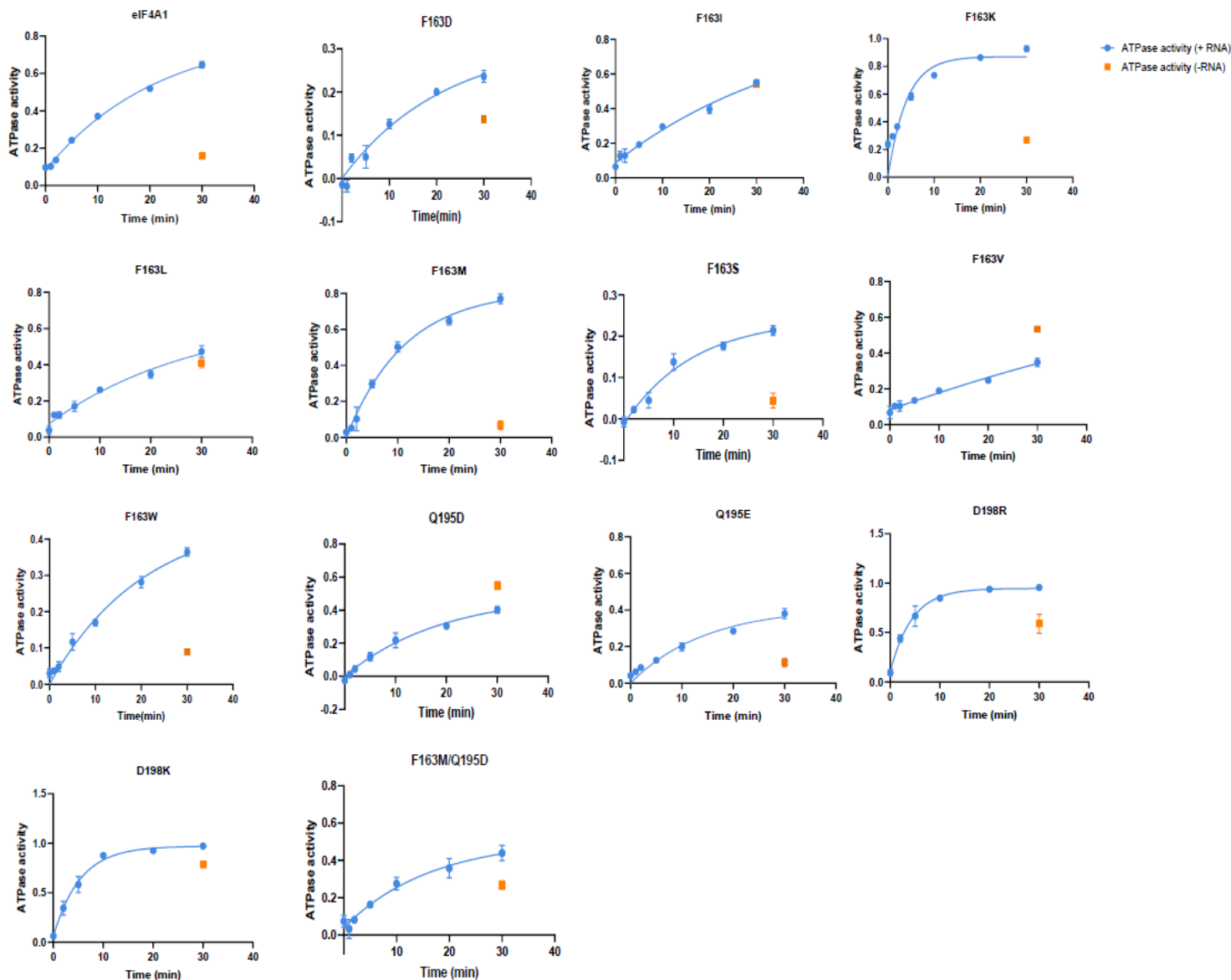


Figure 10: Quantitation of kinetics of ATP hydrolysis by the purified recombinant proteins. ATPase activity was monitored as mentioned above (Figure 9). Activity was quantified by scintillation counts of hydrolyzed and non-hydrolyzed $\gamma\text{-}^{32}\text{P}\text{-ATP}$. ATPase activity was calculated using the following formula: $^{32}\text{P}\text{i counts} / (^{32}\text{P}\text{i counts} + \gamma\text{-}^{32}\text{P}\text{-ATP counts})$. Graphs represent the one-phase association fit showing increase in $\gamma\text{-}^{32}\text{P}\text{-ATP}$ hydrolysis by the proteins with time. Data represents two biological replicates \pm SEM.

3.3 CR-1-31-B stimulates clamping of recombinant proteins onto poly (AG)₈ RNA.

It has been reported previously that rocaglates enhance the RNA binding activity of eIF4A1 [145, 147, 173]. The ability of rocaglates to stimulate the clamping of eIF4A1 onto polypurine RNA has been tested before using Fluorescence Polarization (FP) assay [172, 173]. Taken together, we took an advantage of FP assay (Figure 11a) to assess the ability of CR-1-31-B (Figure 11b) to induce clamping of recombinant proteins onto FAM- poly (AG)₈ RNA in the presence of AMP-PNP (Figure 11c). The change in polarization in presence of compound was compared relative to DMSO control. We chose poly- (AG)₈ RNA as earlier investigations had shown that CR-1-31-B stimulates clamping of eIF4A1 to polypurine enriched RNA sequences over polypyrimidine RNA and that the extent of RNA binding stimulated by CR-1-31-B increased with higher AG content [172]. AMP-PNP, a non-hydrolysable analogue of ATP was used instead of ATP as eIF4A1:poly- (AG)₈ RNA complexes formed by rocaglates are more stable in the presence of AMP-PNP than in the presence of ATP [173]. The concentration of CR-1-31-B and proteins used for the assay were similar to what has been reported by others [145, 172, 174].

Since CR-1-31-B is a potent selective eIF4A inhibitor, we performed the initial clamping assay with this rocaglates to determine its effect on RNA binding by the eIF4A1 mutants. In the absence of compound, we saw that the polarization value obtained with F163W was quite high followed by F163S and F163I proteins. CR-1-31-B was able to increase the binding of eIF4A1, F163K, F163M and F163Y to (AG)₈ RNA after 30 minutes of incubation at RT where eIF4A1 was used as a positive control and showed the expected increase in polarization. In the case of F163K, we attributed the enhanced binding to cation- π interactions induced by lysine (K) with the C-ring of CR-1-31-B. Similarly, in the case of F163M, the sulfur in methionine can potentially form cation- π bond with the aromatic C-ring of CR-1-31-B. Tyrosine (Y) on the other hand forms π -bond with the aromatic ring similar to Phe163 of eIF4A1.

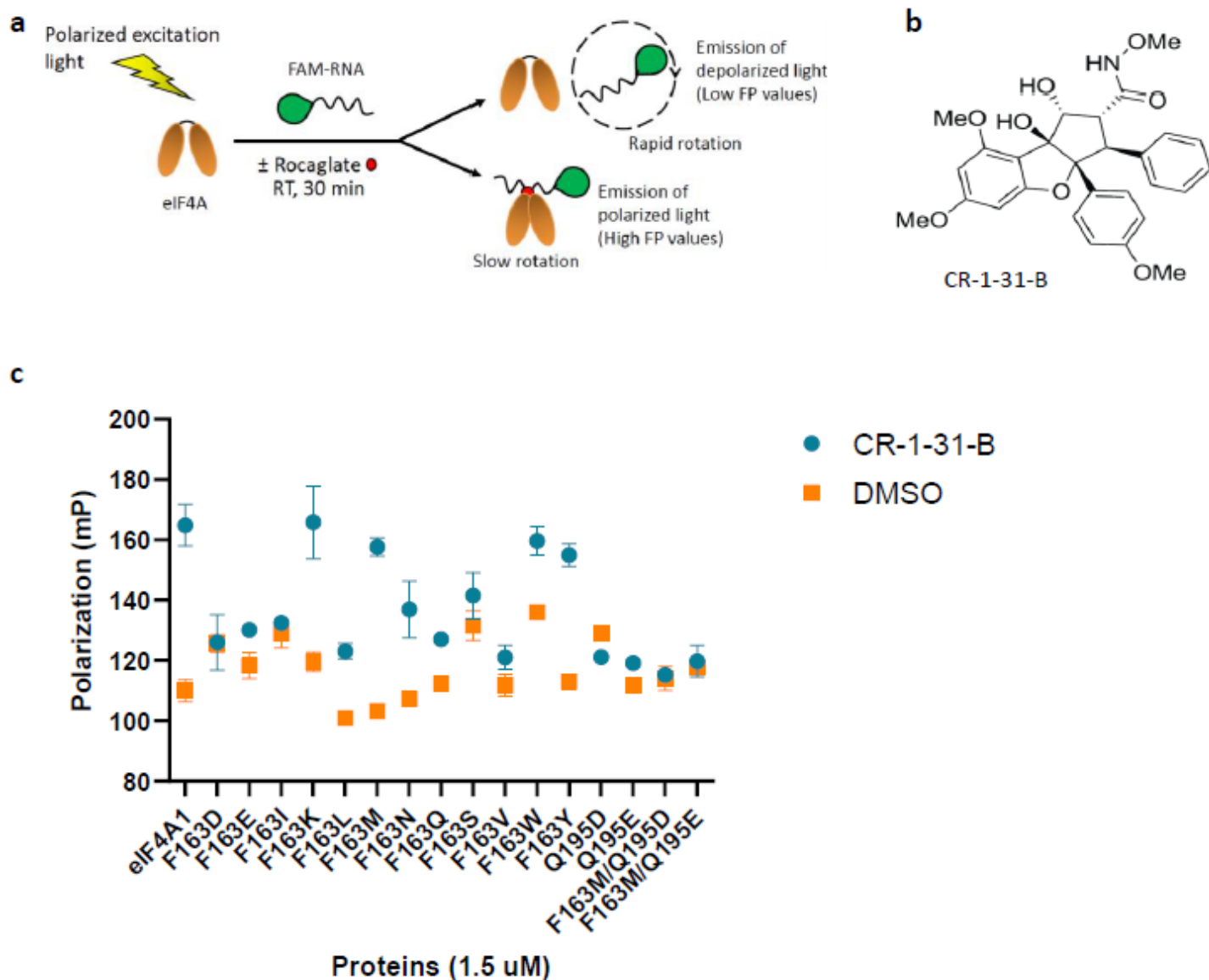


Figure 11: Measuring CR-1-31-B mediated RNA binding of purified proteins. (a) Schematic depicting the principle of Fluorescence Polarization (FP) assay used to determine WT/ mutant-eIF4A1: RNA association. The fluorophore labelled RNA probe is excited by linearly polarized light using a polarization filter. If a compound stimulates binding of protein to the FAM-RNA and stabilizes this complex, it slows the tumbling of the RNA leading to emission of plane polarized light. Contrarily, if there is no clamping and stabilization of protein onto the RNA substrate, the fluorescent probe tumbles leading to emission of depolarized light. (b) Chemical structure of a rocaglate, CR-1-31-B used in this experiment. (c) A plot showing fluorescence polarization values indicating the clamping of eIF4A1/mutant onto the RNA in the presence of CR-1-31-B (shown in green) or DMSO (shown in orange). Briefly, 1.5 μM protein was incubated with 10 nM FAM-poly (AG)₈ RNA and 1 mM AMP-PNP

in the presence or absence of CR-1-31-B for 30 minutes at RT. Data represents 2 biological replicates \pm SD.

Furthermore, F163W and F163N also showed some extent of clamping with RNA as tryptophan and asparagine too can form π -bond. As expected, isoleucine (I) and valine (V) being aliphatic and hydrophobic did not show any stimulated binding with the RNA in presence of CR-1-31-B. Aspartic acid (D) and glutamic acid (E) should theoretically be able to form anionic bond with the aryl-C ring, but we didn't see any extent of RNA binding stimulated by CR-1-31-B with these mutants. Likewise, Q195D and Q195E and the double mutant F163M/Q195D did not show interaction with RNA.

3.4 Comparative assessment of rocaglate mediated WT/ mutant -eIF4A1: RNA clamping.

Since the rocaglate binding site with eIF4A1 is well established and the fact that DDX helicases are conserved throughout the animal kingdom, we wished to explore whether rocaglates can target other DDX proteins. Taking note of interactions of eIF4A1 mutants with CR-1-31-B in the previous experiment, we further wanted to see how different rocaglates behave with these mutants in terms of clamping. We have accumulated a synthetic library of rocaglates with ~390 analogues (BU-CMD collection) synthesized by our collaborator Dr. John Porco at Boston University. We intended to identify if there were any rocaglates in the present BU-CMD collection that were able to selectively clamp a specific mutant eIF4A1 over the WT-eIF4A1. To identify this, we conducted a large-scale screen of this compound library with 13 purified mutant eIF4A1 proteins using FP assay (Figure 13).

Since we aimed to compare and analyze the clamping data of the mutants with wt eIF4A1 to pick out selective rocaglates for the former, we executed the FP screen of F163 and Q195 mutants at same molar concentration as that of eIF4A1. However, in the case of D198R and D198K, when tested at standard FP conditions (1.5 μ M protein), we observed very high polarization values with DMSO alone

(data not shown here). Owing to this, we titrated these proteins at the indicated concentrations (Figure 12) in the presence of 0.1% DMSO and/or CR-1-31-B. Based on the titration curves, the resulting concentrations chosen for D198R and D198K were 390 nM and 218 nM respectively.

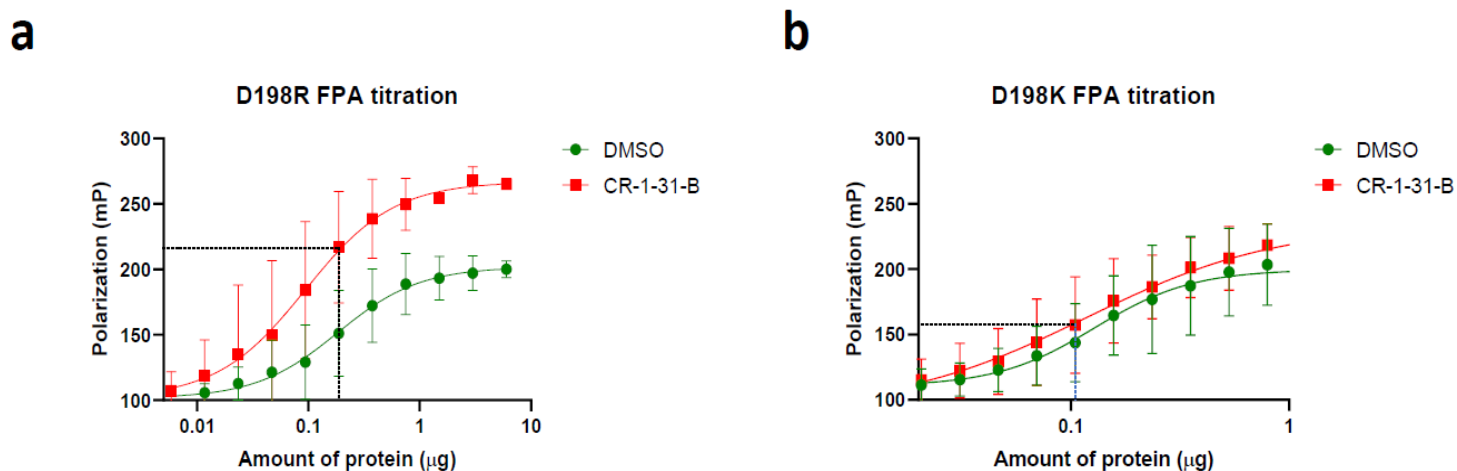
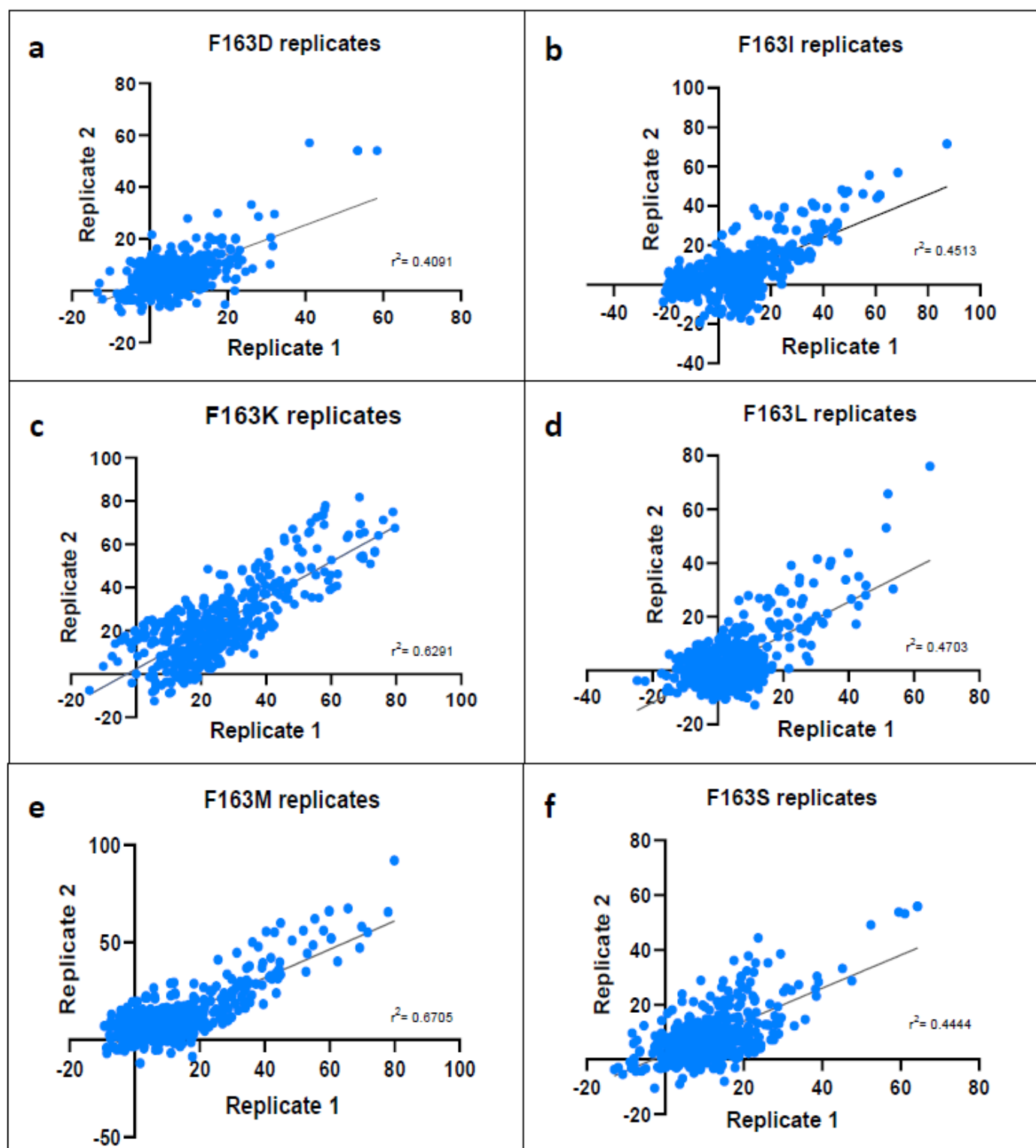
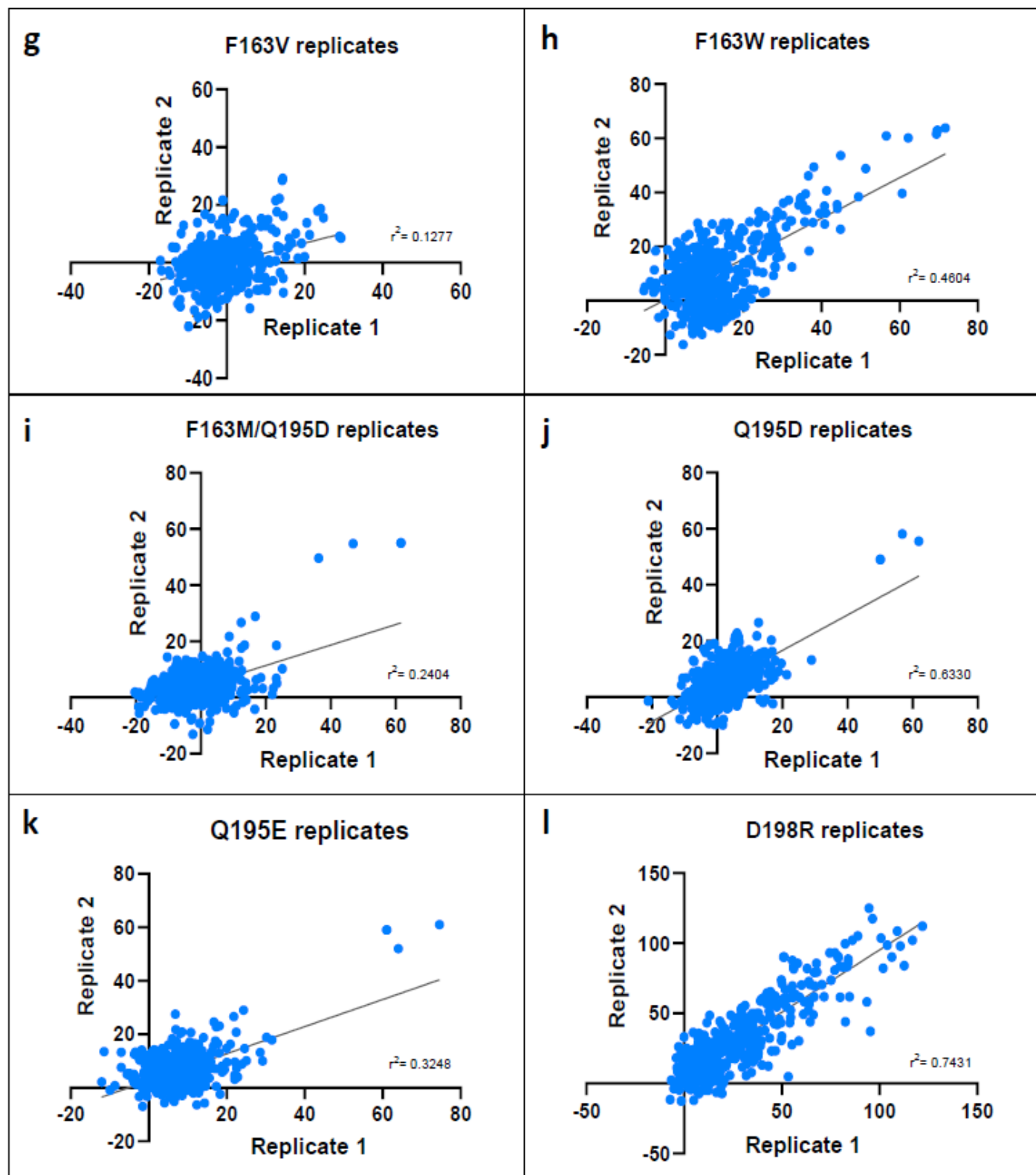


Figure 12: Protein titrations to fix the working concentration in FP assay. The graphs (a, b) represent FAM- poly (AG)₈ RNA binding of the designated proteins at indicated concentrations either in the presence of 10 µM CR-1-31-B (shown in red) or vehicle (0.1% DMSO, which is shown in green). Dotted black lines indicate the chosen concentration at which a large-scale rocaglate screen is conducted. Data represents 3 biological replicates ± SD.

The scatter plots in Figure 13 show the data obtained from high-throughput screening of rocaglates with various recombinant eIF4A1 proteins from two independent experiments. The r^2 value in the scatter plots is a measure of correlation between two independent experiments indicating the replicability of the generated data. Based on the r^2 value, F163K, F163M and D198R show good replicability of the data points (where $r^2 \geq 0.7$). However, in other cases such as F163V, Q195D, Q195E, F163M/Q195D, the lower r^2 values obtained do not suggest non-replicability of the replicates but are rather so due to clustered data points near the origin that show lower or no stimulated binding of proteins to the RNA in the presence of compounds.





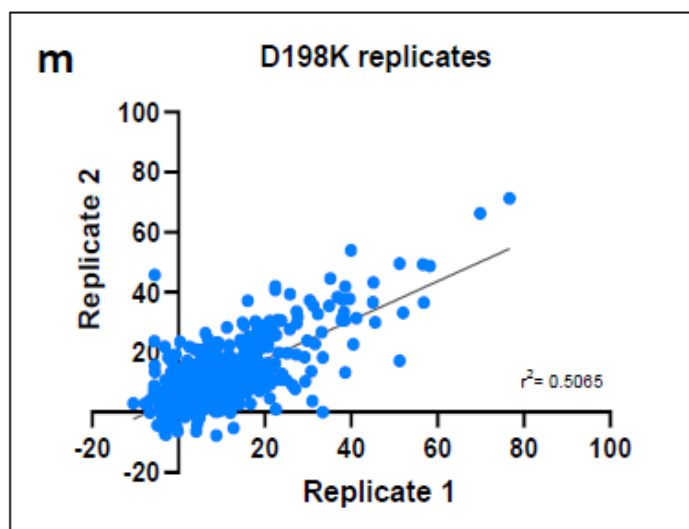
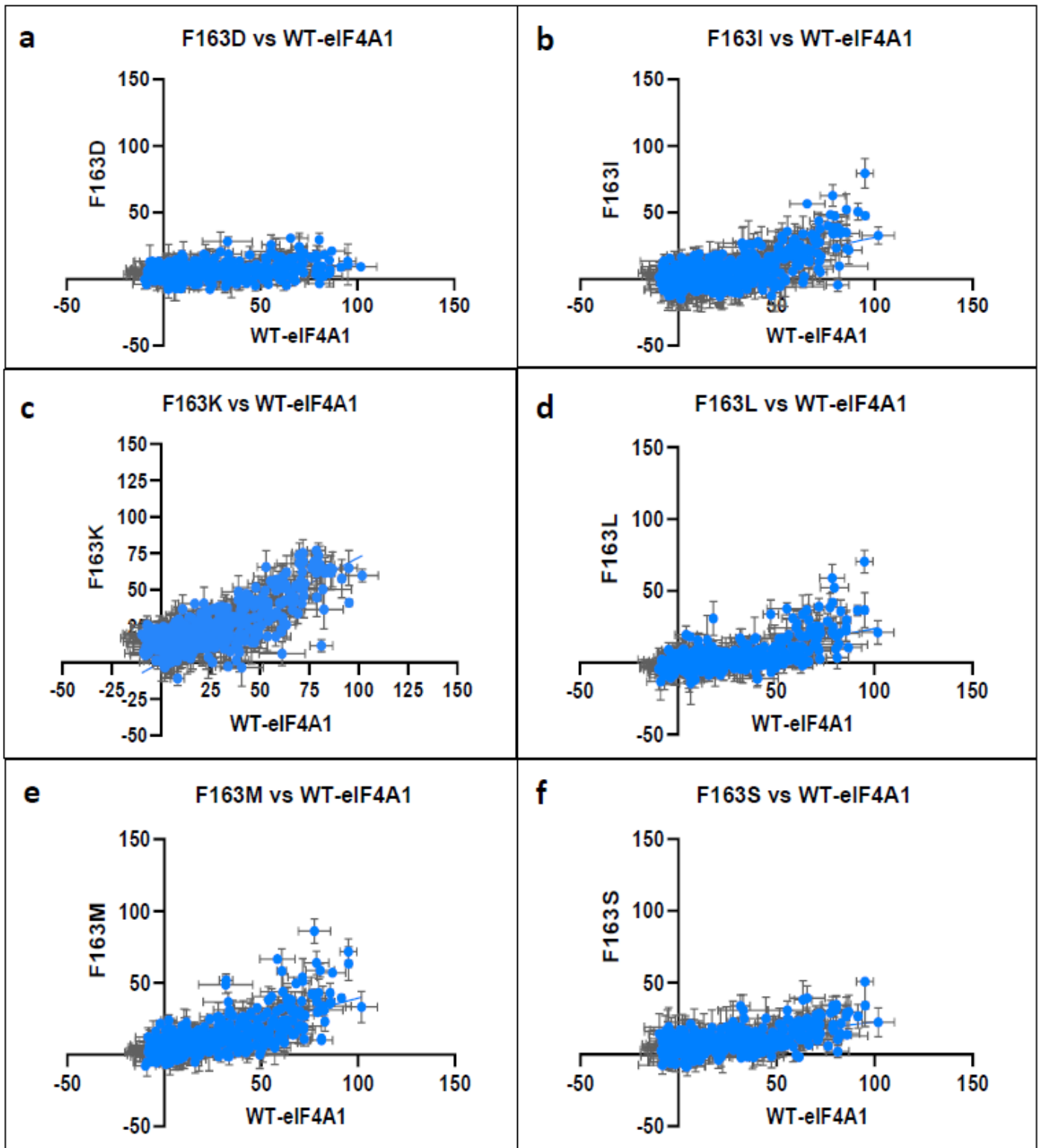
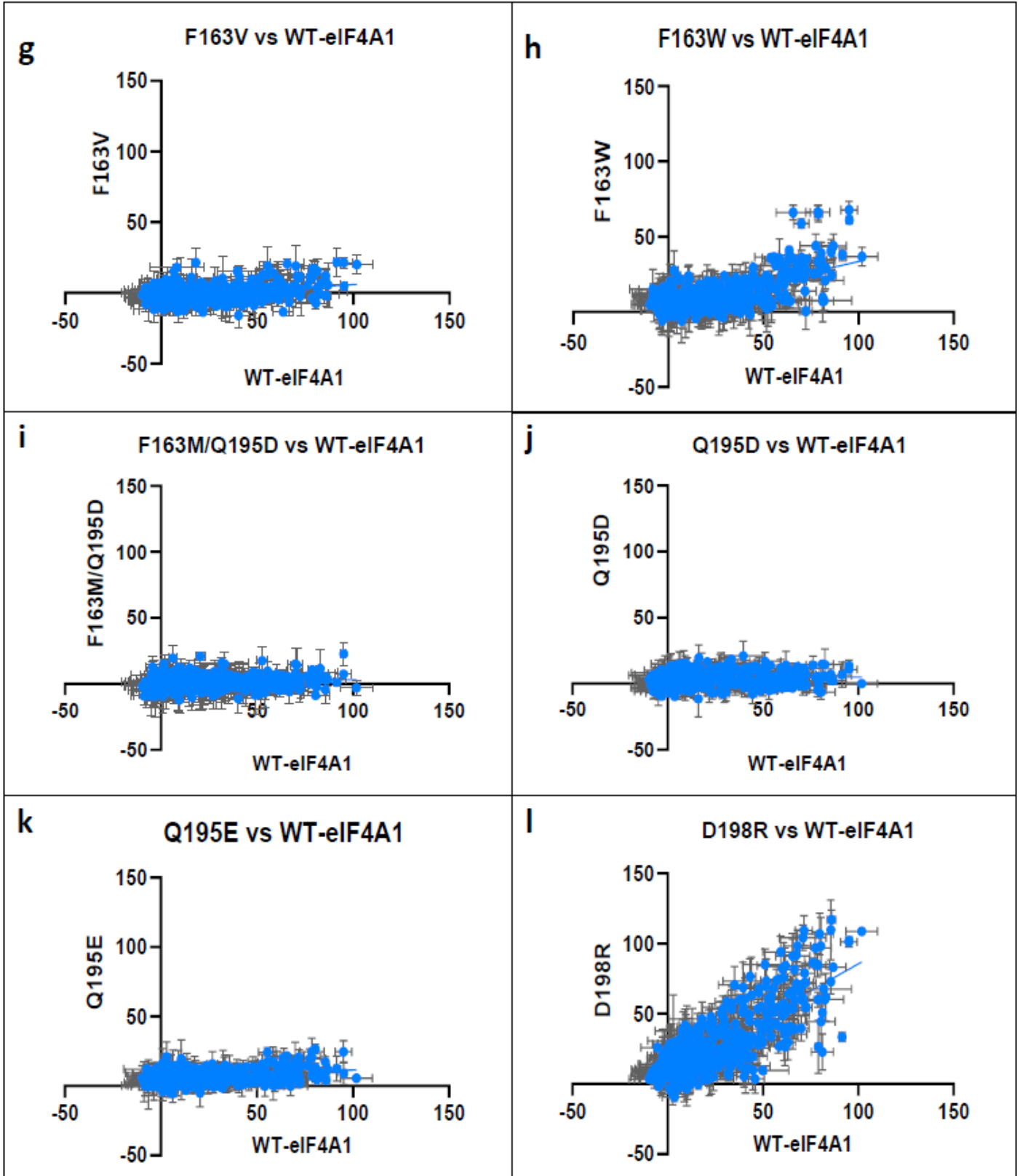


Figure 13: Measuring eIF4A1 mutants:FAM- poly (AG)₈ RNA binding by rocaglates using FP assay. The values are expressed relative to DMSO control. Data represents the correlation between two biological replicates.

Next, we compared the RNA clamping data of these mutants with wt eIF4A1 to see if any compound was selective towards the eIF4A1 mutant (Figure 14). The rocaglate screening data with wt eIF4A1 used for analysis over here was generated by Sai Kiran Naineni (a graduate student in lab). Predominantly, nearly all mutants exhibited lower RNA clamping activity with rocaglates when compared to the wt eIF4A1. However, the RNA binding data with F163K and D198R resembled with wt eIF4A1. This trend in F163K could be due to the cation- π interaction formed by lysine with the C-ring of rocaglates as stated earlier. Similarly, the enhanced binding with D198R could be due to the fact that the two key interacting amino acids, F163 and Q195 in eIF4A1 responsible for rocaglate binding are still present. In addition, the D198 residue in eIF4A1, which lies near the rocaglate binding site is replaced with arginine residue (has a longer side chain) that could bring it closer to rocaglates to stabilize binding (Figure 15).





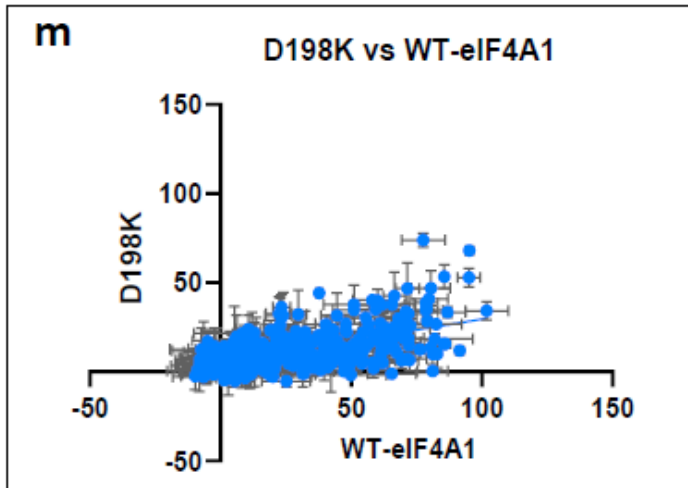


Figure 14: Comparative evaluation of rocaglates stimulated RNA binding of wt eIF4A1 vs mutant eIF4A1. The values are expressed relative to DMSO control. Data represents two biological replicates \pm SEM.

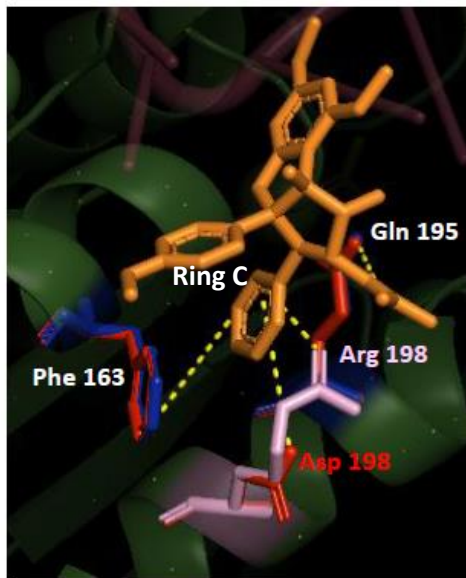


Figure 15: Structural basis for potential interactions between rocaglates and D198R mutant. The figure shows an overlay of eIF4A1 (shown in red) with D198R (shown in light pink) mutant obtained by Swiss-modelling and these proteins are bound to RocA (shown in orange). The interactions are shown in

yellow-dashed lines. Ring C and the C₂ group of RocA interact with F163 and Q195 of eIF4A1 and D198R mutant.

Most of the small molecules in the compound library that showed increased change in polarization with the recombinant proteins, were not specific for the mutant and also targeted wt eIF4A1. Amongst these, CMLD012028, CMLD012824, CMLD012611 and CMLD013366 demonstrated promiscuous activity and were able to bind to many of the tested mutants (Figure 16). We uncovered five compounds, CMLD013163 that presented some degree of specificity towards F163K (Figure 17a) and CMLD012319, BUCMD00002, BUCMD00562 and BUCMD00565 towards D198R over WT-eIF4A1 (Figure 17b). These results remain to be validated.

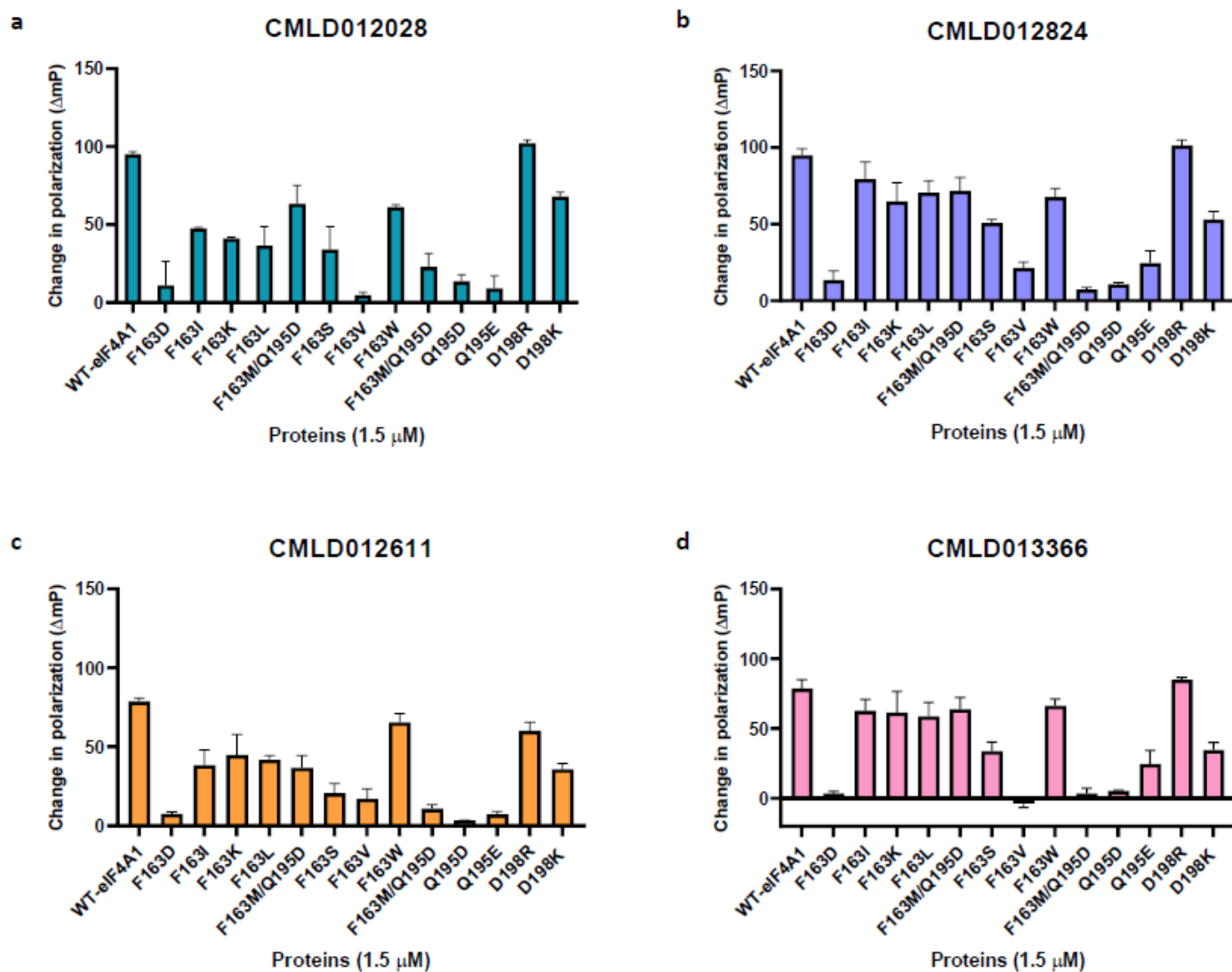


Figure 16: Rocaglates showing promiscuous activity in clamping assay. Each graph compares the clamping of different mutants to poly (AG)₈ RNA in the presence of the indicated compound. In essence, all four compounds induce clamping of all mutants onto this RNA to different extents, with the least being F163D, F163V, F163M/Q195D, Q195D and Q195E. The values are expressed relative to DMSO control. Data represents two biological replicates ± SEM.

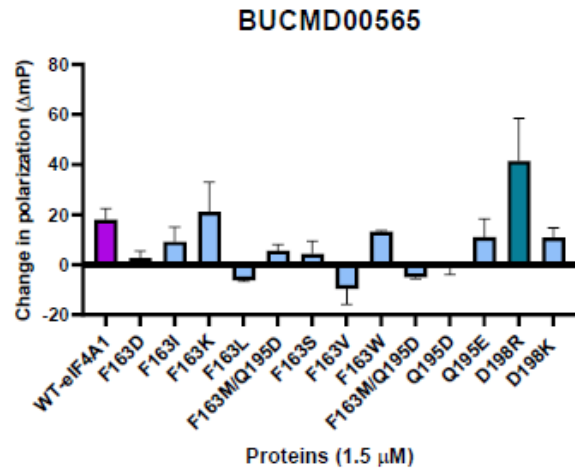
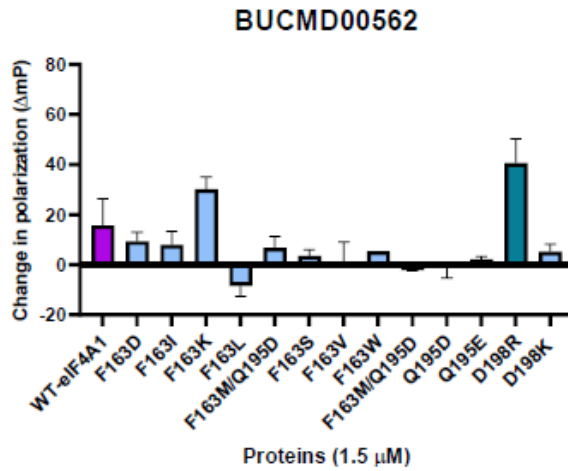
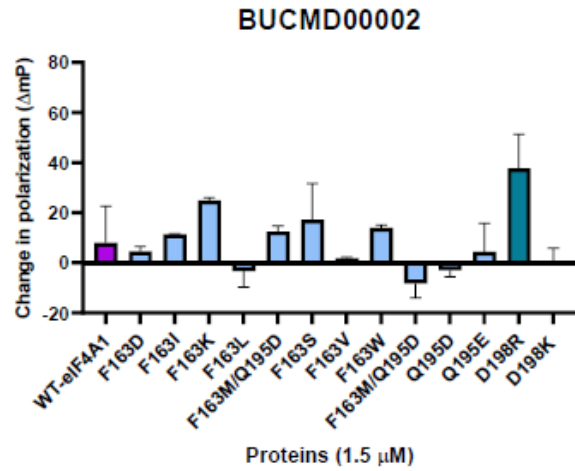
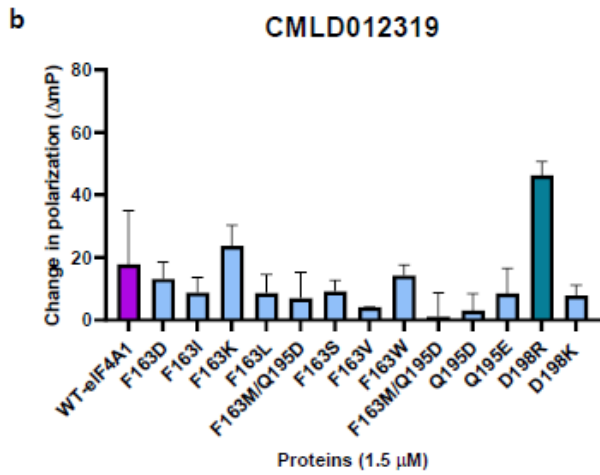
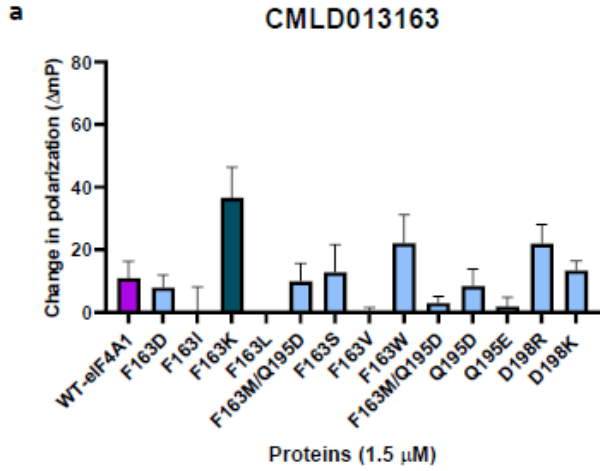


Figure 17. Rocaglates exhibiting specificity towards eIF4A1 mutants. (a) CMLD013163 shows binding preference for F163K over WT-eIF4A1 and other mutants. (b) Compounds showing binding preference for D198R over WT-eIF4A1 and other mutants. The values are expressed relative to DMSO control. Data represents two biological replicates \pm SEM.

4. DISCUSSION

Dysregulation of DNA and RNA helicase can sometimes lead to disease [10, 15, 104, 115, 150, 175-178]. For example, DNA helicases in RecQ and Fe-S families play a vital role in DNA repair and response to replication stress and hence play a prominent role in genome stability and cellular homeostasis [178]. Mutations in genes from these helicase families are linked to cancer progression, and hence present as potential therapeutic targets [178, 179]. For instance, three out of five RecQ family DNA helicases are implicated in genetic diseases that predispose to cancer: *BLM* in Bloom syndrome [180], *WRN* in Werner syndrome [181] and *RECQL4* in Rothmund-Thomson syndrome (RTS) [182]. Individuals affected by these diseases are often diagnosed with a variety of cancers at earlier stages in life as compared to normal individuals [183]. It has been previously reported that conditional silencing of WRN in MYC overexpressing NSCLC xenografts impairs tumor growth [183, 184]. Thus, targeting WRN may help combat MYC-associated tumors. Recently, a small molecule (NSC 19630) was identified to inhibit WRN helicase activity *in vitro* and induce apoptosis in human cancer cells in a WRN-dependent manner [185]. Several efforts are being made in the development of various DNA helicase inhibitors to repair DNA damage and inhibit tumor development [179, 185-187]. Over the recent years, there has been increased interest in association between dysregulation of DDX helicases (RNA helicases) and cancer and notable efforts have been made in developing small molecules to target these helicases [104]. For instance, DDX1 is said to be involved in tumor growth in retinoblastomas [188], neuroblastomas [189-192] and glioblastomas [193]. DDX3X has become a molecule of interest in cancer biology as its overexpression has been implicated in HNSCC [176, 194], lung cancer [195], breast cancer [116, 196] and several others [118, 197-199]. Hence, developing small molecule inhibitors against these DEAD-box proteins offers us with a great opportunity to design and develop novel therapeutics for the treatment of cancers. One crucial

characteristic of tumor forming cells is an increment in translation of various oncogenic transcripts leading to synthesis of oncogenic proteins. Several helicases like DDX2, DDX3X, DDX4 and others are involved in translation. mRNA translation is a finely tuned process and is the most energetically expensive stage in gene expression [69]. Dysregulation in protein synthesis has profound implications on cell fate and can lead to a wide range of disorders including cancer, neurological disorders, viral infections, and diabetes [110, 114, 200-204]. In particular, malignant cells often present with propensity towards elevated protein synthesis to fulfill their requirements for uncontrolled cell division and proliferation [205, 206]. Targeting the protein synthesis machinery thus offers a promising therapeutic strategy for the treatment of these maladies. Over the years, much progress has been made in the development of translation inhibitors by extending the efforts from designing elongation blockers (CHX, HHT, LTM, emetine) to translation initiation inhibitors (rocaglates, hippuristanol and pateamine A). Protein synthesis is mainly regulated at the initiation stage, which is the rate-limiting step amongst the four steps of translation. The major regulators at this step are none other than translation initiation factors [207]. Formation of eIF4F complex is a rate-limiting step and plays a central role in cap-dependent translation initiation. Its mis-regulation has been implicated in several malignancies leading to expression of select mRNAs involved in tumorigenesis and metastasis [208]. Three natural small molecules targeting eIF4A have been identified and studied to date, namely rocaglates, hippuristanol and pateamine A. Hippuristanol allosterically inhibits the binding of both bound and unbound eIF4A to RNA and blocks its helicase as well as ATPase activities [130]. On the other hand, rocaglates and Pateamine A increase the RNA-binding capability of eIF4A leading to hinderance in eIF4F complex formation by RNA-mediated eIF4A sequestration. However, Pateamine A is a potent inhibitor of translation and shows high toxicity *in vivo* [209]. Because of this, rocaglates have our particular interest owing to their potency in both *in vitro* and *in vivo* settings and are well tolerated *in vivo*. Moreover, there is strong evidence suggesting that rocaglates (i.e., silvestrol) are

capable of chemo-sensitizing drug resistant tumors in E μ -myc mice lymphoma models [142]. Taken together, rocaglates seem to be powerful clinical candidates to shut down protein synthesis in cancerous cells.

Structural basis of rocaglate binding with eIF4A1 and poly- (AG)₅ RNA in the presence of AMP-PNP is very well established by Iwasaki et al., [147] and is dependant on F163 and Q195 amino acids in eIF4A1 at these locations (Figure 6a). Given that DDX helicase cores are conserved throughout the animal kingdom, we were interested in the possibility of broadening the targeting spectrum of rocaglates from selective eIF4A inhibitors to other DDX proteins by making structural modifications in them. Thus, we aligned the functionally conserved sequences of mammalian DDX proteins with that of eIF4A1 and identified the amino acid diversity present at F163 and Q195 positions of eIF4A1 in these helicases. Only human eIF4A proteins have the F163 and Q195 amino acid combination, with the rest of the helicases having different amino acid combinations at these positions. This presents us with a wonderful advantage to target these helicases by altering rocaglates- selective interfacial eIF4A1 inhibitors. Taking a step forward in this direction, we along with our collaborators at Boston University, took an initiative to screen compounds with different functional groups that might alter their binding specificity towards these DEAD-box RNA helicases.

Firstly, we made mutations in eIF4A1 protein sequence at either F163 and/ or Q195 positions and substituted them with the amino acids found in the DDX of interest. Apart from these, two additional mutant eIF4A1 namely, D198R and D198K were also generated. D198 in eIF4A1 lies near the rocaglate binding site (Figure 6a). Considering this, if we substitute the aspartate with either arginine (R) or lysine (K), both of which contain a long side chain, we could potentially induce electrostatic interactions with rocaglates as they might come in the vicinity of rocaglate binding site. Moreover, DDX3X possesses an

arginine (R) residue at D198 of eIF4A1 whereas DDX5 and DDX17 possess lysine at D198. In addition to this, these mutants were of interest as their corresponding helicases are involved in tumorigenesis: DDX3X is expressed in various carcinomas, whereas DDX5 and DDX17 are overexpressed in most tumors such as breast cancer [210, 211], NSCLC [18, 212], prostate cancer [34, 213], endometrial cancer [214] and many more [215-222].

It is well-known that eIF4A1 possesses ATP-dependent RNA helicase and RNA-dependent ATPase activities. An activated closed conformer of eIF4A hydrolyzes ATP and releases the unwound RNA strand. Based on this fact, we deduced that our purified protein preparations were functionally active based on their ability to hydrolyze ATP in the presence of RNA. We saw an increase in the release of $^{32}\text{P}_i$ by WT- and mutant eIF4A1 proteins with increasing time in the presence of poly- (U) RNA for up to 20-30 minutes, which we would expect if they were functionally active from our previous studies (Figure 9, 10).

We have accumulated a synthetic library of rocaglates with around 390 analogues (BU-CMD collection) synthesized by our collaborator Dr. John Porco and his team at Boston University. This compound library is a result of Dr. Porco and his group's significant efforts in synthesizing rocaglate analogues with alterations at Ar-C ring and 2- N,N-dimethyl carboxamide (the C₂ carbonyl group), the two moieties that are responsible for interacting with F163 and Q195 respectively. We intended to identify if there were any rocaglates in the present BU-CMD collection that were able to selectively clamp a specific mutant eIF4A1 over wt eIF4A1. To identify this, we tested the compound library with 13 of our purified mutant eIF4A1 proteins using the FP assay, as mentioned earlier. We compared the compound clamping data of these mutants with that of wt eIF4A1 to see if any compound was selective towards the mutant.

From this screen, we identified four compounds that showed binding activity with most of the mutants tested in FP assay and appeared to be more promiscuous (Figure 16). All four compounds induced significant clamping of the D198R mutant to RNA, to a level comparable as eIF4A1. Of these four compounds, CMLD012611, CMLD012824, and CMLD013366 are amidino-rocaglates (CMLD012824 and CMLD013366 are same compounds but from two different batches). The reason for this increased promiscuity is not completely understood and awaits further experiments.

We did not find any rocaglate analogue showing specific activity towards any of our mutant proteins except for the F163K and D198R mutants, where there were five compounds that showed activity. CMLD013163 (Figure 17a) showed some specificity towards F163K over WT-eIF4A1, however, it is noteworthy that the RNA binding with F163K caused by this compound was not very robust. The change in polarization obtained with F163K ($\Delta mP=37$) was twice than what we observed for eIF4A1 ($\Delta mP=11$). This compound differs from RocA, a prototype rocaglamide by the presence of a chloride group at the para position on ring C and a methoxycarbonyl group at C₂ instead of a tertiary amide. The chloride group at the C ring acts as an electron donating group and is an activating group that increases the electron density of the aromatic ring. The electron rich C ring could in principle form strong cation- π interaction with the protonated amino group in lysine of F163K which could explain the stronger interaction of this compound with F163K, compared to phenylalanine which makes a π - π interaction. Moreover, the oxygen at C₂ carbonyl group forms a hydrogen bond with hydrogen in -NH₂ of glutamine at 195 position. We also noticed that change in stereochemistry of C-ring and C₂ carbonyl group and increasing the distance of the C-ring from the cyclopentane ring by two carbons diminished the clamping of F163K to poly-(AG)₈, which was the case with CMLD013166 - a congener of CMLD013163. Another structurally similar compound CMLD013164 with stereochemistry similar to CMLD013163 but differed by presence of

carboxamide at C₂ position and 4-methoxy moiety at ring C showed a lower degree of clamping to F163K but no clamping with WT-eIF4A1. This could be because chlorine is a stronger electron donating group (EDG) than methoxy, meaning it can increase the electron density at ring C which results in stronger interaction with lysine (of F163K). Taken together, it suggests that maybe enhancing the electron density at C-ring of rocaglates with an altered stereochemistry of the ring B (which is seen in CMLD013163 and CMLD013164 that showed some clamping to F163K over WT-eIF4A1) which stacks with guanine base of G8 [147] might result in compound selectivity towards F163K.

CMLD012319 is a rocaglate with a 2-(*m-tolyl*)pyrimidin-4(3*H*)-one moiety fused with the cyclopentane ring of the structural backbone that showed specificity towards D198R ($\Delta mP = 49.95$) (Figure 17b). Substituting this pyrimidinone ring with *o*-chlorobenzene (CMLD012318) instead of *m*-toluene or increasing the distance of benzene ring from pyrimidinone moiety by one carbon (i.e. 2-benzylpyrimidin-4(3*H*)-one) in CMLD012320 reduced and diminished the selectivity of compound towards D198R and showed comparatively stronger interaction with wt eIF4A1. Two other compounds BUCMD00562 and BUCMD00565 with 3,4-*o*-difluoro and 3,5-*m*-difluoro group respectively at Ar-C ring and a methoxycarbonyl group at C₂ showed binding preference to D198R as opposed to WT-eIF4A1 (Figure 17b). It is possible that this interaction is observed because of potential electrostatic interaction between partially positive portion of guanidino group in arginine and the electron rich C ring (which in this case is the result of fluoride group on ring C that acts as an EDG). An interesting observation here was that if the compound is substituted with just 2-fluoro at ring C (BUCMD00569), it exhibits no binding with D198R but rather shows good clamping with eIF4A1. Altering the position of halogens at C ring negatively affects the clamping of compound to both D198R and wt protein (BUCMD00561, BUCMD00564). Altering the stereochemistry of compound and changing the methoxycarbonyl group to

carboxamide (BUCMD00566, BUCMD00567) shows no clamping to either of the proteins. Another result was that BUCMD00002 which has a modified B ring (brominated at para position) and possesses a methoxycarbonyl moiety at C2 exhibits selectivity towards D198R although with an intermediate degree clamping ($\Delta mP=37.7$). This was interesting because substituting the C2 group in this compound with carboxamide (BUCMD00003, CMLD010508) renders the compound non-specific and exhibits binding with WT-eIF4A1 and D198R.

In addition to the eIF4A1 mutants, we also cloned the DDX20 helicase core (data not shown) since we had previously tested DDX21 and DDX50 with the rocaglate library (tested by Sai Kiran Naineni, data not shown) and all the three helicases possess F163K residue. Since we had rocaglate binding data with F163K, we were interested in comparing and assessing the rocaglate activity profile of F163K with its corresponding helicases. Hence, we purified DDX20 and tested the rocaglate library with the same and checked if CMLD013163 showed any selectivity to either of these helicase cores over WT-eIF4A1 or not as it showed preference for F163K mutant in our screen. Unfortunately, neither of these helicases showed good RNA binding with this compound. In fact, no compound from the library showed any selectivity to the DDX20, DDX21, or DDX50 helicase cores. Another important point to note was that in general, not all the compounds that showed good clamping with F163K exhibited the same behaviour with DDX20, DDX21 and DDX50. The RNA binding capability of these helicase cores in the presence of a rocaglate was relatively lower than what was obtained with F163K. Similarly, the RNA binding data of F163V and D198R was compared with DDX3 (data not shown) as the latter has valine and arginine present at 163 and 198 position of eIF4A1 respectively. No compound displayed discrimination towards DDX3X which was consistent with the F163V screening data. However, the four compounds that exhibited some degree of selectivity towards D198R did not clamp DDX3X to RNA. The reason why this behaviour was seen

could be because although the mutations made in eIF4A1 correspond to the key interacting amino acids in the DDX helicase cores, these mutants do not actually represent the entire helicase core. It is very likely that the 3D arrangement of actual full-length DEAD-box helicases is different than eIF4A1 mutants and that their binding pocket is different.

Overall, all the findings from the work described here indicate that no rocaglate was found capable of selectively clamping our generated single mutants onto poly (AG)₈ RNA. When compared to the clamping data available for the corresponding DEAD-box helicases, no compound was found to be selective towards the respective helicase core. However, it might be worth to further optimize the structures of compounds that exhibited a certain degree of selectivity towards F163K and D198R. Should they show any bias towards the mutant, future experiments must be performed to check if these compounds are able to bind their respective helicase cores. Structural characterization must be undertaken for potential new DDX•AMP-PNP•rocaglate•poly r(AG)₅ complex to determine the exact interaction sites and to identify the positions at which rocaglates could be further modified to optimize their binding with the DEAD-box helicase of interest.

5. CONCLUSION

Through structure-based drug design and chemical biology approach, we screened for functional groups in rocaglates with the aim to broaden their spectrum of activity from eIF4A1 to other DEAD-box RNA helicases that are implicated in various types of cancers. Taking advantage of a fluorescence polarization (FP) assay, we tested the designed rocaglates to assess their clamping activity with various mutant eIF4A1 proteins that were engineered to mimic the interacting sites of the corresponding helicase cores. We identified five rocaglates that showed binding preference to two of our eIF4A1 mutants from our large-scale screen. Structural insights into rocaglates would help us further modify their structure for optimal and efficient binding to the DEAD-box helicase of interest.

REFERENCES

1. Lohman, T.M., E.J. Tomko, and C.G. Wu, *Non-hexameric DNA helicases and translocases: mechanisms and regulation*. Nature Reviews Molecular Cell Biology, 2008. **9**(5): p. 391-401.
2. Pyle, A.M., *Translocation and unwinding mechanisms of RNA and DNA helicases*. Annu. Rev. Biophys., 2008. **37**: p. 317-336.
3. Singleton, M.R., M.S. Dillingham, and D.B. Wigley, *Structure and mechanism of helicases and nucleic acid translocases*. Annu Rev Biochem, 2007. **76**: p. 23-50.
4. Anantharaman, V., E.V. Koonin, and L. Aravind, *Comparative genomics and evolution of proteins involved in RNA metabolism*. Nucleic acids research, 2002. **30**(7): p. 1427-1464.
5. Frick, D.N. and A. Lam, *Understanding helicases as a means of virus control*. Current pharmaceutical design, 2006. **12**(11): p. 1315-1338.
6. Fairman-Williams, M.E., U.P. Guenther, and E. Jankowsky, *SF1 and SF2 helicases: family matters*. Curr Opin Struct Biol, 2010. **20**(3): p. 313-24.
7. Abdelhaleem, M., *Helicases: an overview*. Methods Mol Biol, 2010. **587**: p. 1-12.
8. Pang, P.S., et al., *The hepatitis C viral NS3 protein is a processive DNA helicase with cofactor enhanced RNA unwinding*. Embo j, 2002. **21**(5): p. 1168-76.
9. Boulé, J.B. and V.A. Zakian, *The yeast Pif1p DNA helicase preferentially unwinds RNA DNA substrates*. Nucleic Acids Res, 2007. **35**(17): p. 5809-18.
10. Jankowsky, E., *RNA helicases at work: binding and rearranging*. Trends Biochem Sci, 2011. **36**(1): p. 19-29.
11. Tanner, N.K. and P. Linder, *DEAD/H box RNA helicases: from generic motors to specific dissociation functions*. Mol Cell, 2001. **8**(2): p. 251-62.
12. Rocak, S. and P. Linder, *DEAD-box proteins: the driving forces behind RNA metabolism*. Nature reviews Molecular cell biology, 2004. **5**(3): p. 232-241.
13. Russell, R., I. Jarmoskaite, and A.M. Lambowitz, *Toward a molecular understanding of RNA remodeling by DEAD-box proteins*. RNA biology, 2013. **10**(1): p. 44-55.
14. Putnam, A.A. and E. Jankowsky, *DEAD-box helicases as integrators of RNA, nucleotide and protein binding*. Biochimica et Biophysica Acta (BBA)-Gene Regulatory Mechanisms, 2013. **1829**(8): p. 884-893.
15. Ali, M.A.M., *The DEAD-box protein family of RNA helicases: sentinels for a myriad of cellular functions with emerging roles in tumorigenesis*. International Journal of Clinical Oncology, 2021. **26**(5): p. 795-825.
16. Tanner, N.K., *The Newly Identified Q Motif of DEAD Box Helicases IS Involved in Adenine Recognition*. Cell Cycle, 2003. **2**(1): p. 18-19.
17. Bono, F., et al., *The crystal structure of the exon junction complex reveals how it maintains a stable grip on mRNA*. Cell, 2006. **126**(4): p. 713-25.

18. Yang, Z., et al., *Molecular Insights into the Recruiting Between UCP2 and DDX5/UBAP2L in the Metabolic Plasticity of Non-Small-Cell Lung Cancer*. Journal of Chemical Information and Modeling, 2021. **61**(8): p. 3978-3987.
19. Linder, P., N.K. Tanner, and J. Banroques, *From RNA helicases to RNPases*. Trends in biochemical sciences, 2001. **26**(6): p. 339-341.
20. Cordin, O., et al., *The DEAD-box protein family of RNA helicases*. Gene, 2006. **367**: p. 17-37.
21. Samatanga, B., A.Z. Andreou, and D. Klostermeier, *Allosteric regulation of helicase core activities of the DEAD-box helicase YxiN by RNA binding to its RNA recognition motif*. Nucleic Acids Research, 2017. **45**(4): p. 1994-2006.
22. Theissen, B., et al., *Cooperative binding of ATP and RNA induces a closed conformation in a DEAD box RNA helicase*. Proc Natl Acad Sci U S A, 2008. **105**(2): p. 548-53.
23. Hilbert, M., A.R. Karow, and D. Klostermeier, *The mechanism of ATP-dependent RNA unwinding by DEAD box proteins*. 2009. **390**(12): p. 1237-1250.
24. Henn, A., et al., *Pathway of ATP utilization and duplex rRNA unwinding by the DEAD-box helicase, DbpA*. Proceedings of the National Academy of Sciences, 2010. **107**(9): p. 4046-4050.
25. Liu, F., A. Putnam, and E. Jankowsky, *ATP hydrolysis is required for DEAD-box protein recycling but not for duplex unwinding*. Proc Natl Acad Sci U S A, 2008. **105**(51): p. 20209-14.
26. Shen, L. and J. Pelletier, *General and Target-Specific DExD/H RNA Helicases in Eukaryotic Translation Initiation*. International Journal of Molecular Sciences, 2020. **21**(12): p. 4402.
27. Andersen, C.B., et al., *Structure of the exon junction core complex with a trapped DEAD-box ATPase bound to RNA*. Science, 2006. **313**(5795): p. 1968-1972.
28. Jarmoskaite, I. and R. Russell, *RNA helicase proteins as chaperones and remodelers*. Annual review of biochemistry, 2014. **83**: p. 697.
29. Schütz, P., et al., *Comparative structural analysis of human DEAD-box RNA helicases*. PloS one, 2010. **5**(9): p. e12791.
30. Yang, Q., et al., *DEAD-box proteins unwind duplexes by local strand separation*. Mol Cell, 2007. **28**(2): p. 253-63.
31. Yang, Q. and E. Jankowsky, *The DEAD-box protein Ded1 unwinds RNA duplexes by a mode distinct from translocating helicases*. Nat Struct Mol Biol, 2006. **13**(11): p. 981-6.
32. Bourgeois, C.F., F. Mortreux, and D. Auboeuf, *The multiple functions of RNA helicases as drivers and regulators of gene expression*. Nature reviews Molecular cell biology, 2016. **17**(7): p. 426-438.
33. Bates, G.J., et al., *The DEAD box protein p68: a novel transcriptional coactivator of the p53 tumour suppressor*. The EMBO Journal, 2005. **24**(3): p. 543-553.
34. Clark, E.L., et al., *The RNA helicase p68 is a novel androgen receptor coactivator involved in splicing and is overexpressed in prostate cancer*. Cancer research, 2008. **68**(19): p. 7938-7946.
35. Wagner, M., et al., *DDX5 is a multifunctional co-activator of steroid hormone receptors*. Molecular and Cellular Endocrinology, 2012. **361**(1): p. 80-91.

36. Watanabe, M., et al., *Retracted: A subfamily of RNA-binding DEAD-box proteins acts as an estrogen receptor α coactivator through the N-terminal activation domain (AF-1) with an RNA coactivator, SRA*. The EMBO journal, 2001. **20**(6): p. 1341-1352.
37. Wang, R., et al., *P68 RNA helicase promotes invasion of glioma cells through negatively regulating DUSP5*. Cancer Sci, 2019. **110**(1): p. 107-117.
38. Yang, L., C. Lin, and Z.R. Liu, *P68 RNA helicase mediates PDGF-induced epithelial mesenchymal transition by displacing Axin from beta-catenin*. Cell, 2006. **127**(1): p. 139-55.
39. Wilson, B.J., et al., *The p68 and p72 DEAD box RNA helicases interact with HDAC1 and repress transcription in a promoter-specific manner*. BMC Molecular Biology, 2004. **5**(1): p. 11.
40. Calo, E., et al., *RNA helicase DDX21 coordinates transcription and ribosomal RNA processing*. Nature, 2015. **518**(7538): p. 249-53.
41. Polprasert, C., et al., *Inherited and Somatic Defects in DDX41 in Myeloid Neoplasms*. Cancer Cell, 2015. **27**(5): p. 658-70.
42. Ilagan, J.O., et al., *Rearrangements within human spliceosomes captured after exon ligation*. Rna, 2013. **19**(3): p. 400-12.
43. Wang, Z., V. Murigneux, and H. Le Hir, *Transcriptome-wide modulation of splicing by the exon junction complex*. Genome Biology, 2014. **15**(12): p. 551.
44. Lari, A., et al., *A nuclear role for the DEAD-box protein Dbp5 in tRNA export*. eLife, 2019. **8**: p. e48410.
45. Mason, A.C. and S.R. Wentz, *Functions of Gle1 are governed by two distinct modes of self-association*. bioRxiv, 2020.
46. Lai, M.C., Y.H. Lee, and W.Y. Tarn, *The DEAD-box RNA helicase DDX3 associates with export messenger ribonucleoproteins as well as tip-associated protein and participates in translational control*. Mol Biol Cell, 2008. **19**(9): p. 3847-58.
47. Mo, J., et al., *DDX3X: structure, physiologic functions and cancer*. Molecular Cancer, 2021. **20**(1): p. 38.
48. Naineni, S.K., et al., *Targeting DEAD-box RNA helicases: The emergence of molecular staples*. Wiley Interdiscip Rev RNA, 2022: p. e1738.
49. Martin, R., et al., *DExD/H-box RNA helicases in ribosome biogenesis*. RNA Biology, 2013. **10**(1): p. 4-18.
50. Pelletier, J. and N. Sonenberg, *The Organizing Principles of Eukaryotic Ribosome Recruitment*. Annual Review of Biochemistry, 2019. **88**(1): p. 307-335.
51. Hao, P., et al., *Eukaryotic translation initiation factors as promising targets in cancer therapy*. Cell Communication and Signaling, 2020. **18**(1): p. 175.
52. Shen, L. and J. Pelletier, *Selective targeting of the DEAD-box RNA helicase eukaryotic initiation factor (eIF) 4A by natural products*. Nat Prod Rep, 2020. **37**(5): p. 609-616.
53. Chen, H., et al., *DDX3 modulates cell adhesion and motility and cancer cell metastasis via Rac1-mediated signaling pathway*. Oncogene, 2015. **34**(21): p. 2790-2800.

54. Lai, M.-C., et al., *DDX3 regulates cell growth through translational control of cyclin E1*. Molecular and cellular biology, 2010. **30**(22): p. 5444-5453.
55. Soto-Rifo, R., et al., *DEAD-box protein DDX3 associates with eIF4F to promote translation of selected mRNAs*. The EMBO journal, 2012. **31**(18): p. 3745-3756.
56. Guenther, U.-P., et al., *The helicase Ded1p controls use of near-cognate translation initiation codons in 5' UTRs*. Nature, 2018. **559**(7712): p. 130-134.
57. Gupta, N., J.R. Lorsch, and A.G. Hinnebusch, *Yeast Ded1 promotes 48S translation pre-initiation complex assembly in an mRNA-specific and eIF4F-dependent manner*. eLife, 2018. **7**: p. e38892.
58. Calviello, L., et al., *DDX3 depletion represses translation of mRNAs with complex 5' UTRs*. Nucleic Acids Research, 2021. **49**(9): p. 5336-5350.
59. Collier, J.M., et al., *The DEAD box helicase, Dhh1p, functions in mRNA decapping and interacts with both the decapping and deadenylase complexes*. Rna, 2001. **7**(12): p. 1717-27.
60. Fischer, N. and K. Weis, *The DEAD box protein Dhh1 stimulates the decapping enzyme Dcp1*. Embo j, 2002. **21**(11): p. 2788-97.
61. Michelle, L., et al., *Proteins associated with the exon junction complex also control the alternative splicing of apoptotic regulators*. Mol Cell Biol, 2012. **32**(5): p. 954-67.
62. Iwatani-Yoshihara, M., et al., *Discovery and Characterization of a Eukaryotic Initiation Factor 4A-3-Selective Inhibitor That Suppresses Nonsense-Mediated mRNA Decay*. ACS Chemical Biology, 2017. **12**(7): p. 1760-1768.
63. Todd, A.G., et al., *SMN, Gemin2 and Gemin3 associate with beta-actin mRNA in the cytoplasm of neuronal cells in vitro*. J Mol Biol, 2010. **401**(5): p. 681-9.
64. Kanai, Y., N. Dohmae, and N. Hirokawa, *Kinesin transports RNA: isolation and characterization of an RNA-transporting granule*. Neuron, 2004. **43**(4): p. 513-25.
65. Buttgereit, F. and M.D. Brand, *A hierarchy of ATP-consuming processes in mammalian cells*. Biochem J, 1995. **312** (Pt 1)(Pt 1): p. 163-7.
66. Roux, P.P. and I. Topisirovic, *Regulation of mRNA translation by signaling pathways*. Cold Spring Harb Perspect Biol, 2012. **4**(11).
67. Ramon y Cajal, S., et al., *Beyond molecular tumor heterogeneity: protein synthesis takes control*. Oncogene, 2018. **37**(19): p. 2490-2501.
68. Walsh, D. and I. Mohr, *Viral subversion of the host protein synthesis machinery*. Nature Reviews Microbiology, 2011. **9**(12): p. 860-875.
69. Sonenberg, N. and A.G. Hinnebusch, *Regulation of translation initiation in eukaryotes: mechanisms and biological targets*. Cell, 2009. **136**(4): p. 731-45.
70. Gebauer, F. and M.W. Hentze, *Molecular mechanisms of translational control*. Nature Reviews Molecular Cell Biology, 2004. **5**(10): p. 827-835.
71. Jackson, R.J., C.U.T. Hellen, and T.V. Pestova, *The mechanism of eukaryotic translation initiation and principles of its regulation*. Nature Reviews Molecular Cell Biology, 2010. **11**(2): p. 113-127.

72. Gallie, D.R., *The cap and poly(A) tail function synergistically to regulate mRNA translational efficiency*. Genes & development, 1991. **5** **11**: p. 2108-16.
73. Gallie, D.R., *The role of the poly(A) binding protein in the assembly of the Cap-binding complex during translation initiation in plants*. Translation (Austin), 2014. **2**(2): p. e959378.
74. Sonenberg, N., et al., *A polypeptide in eukaryotic initiation factors that crosslinks specifically to the 5'-terminal cap in mRNA*. Proc Natl Acad Sci U S A, 1978. **75**(10): p. 4843-7.
75. Hernández, G. and P. Vazquez-Pianzola, *Functional diversity of the eukaryotic translation initiation factors belonging to eIF4 families*. Mechanisms of Development, 2005. **122**(7): p. 865-876.
76. Matsuo, H., et al., *Structure of translation factor eIF4E bound to m7GDP and interaction with 4E-binding protein*. Nat Struct Biol, 1997. **4**(9): p. 717-24.
77. Tomoo, K., et al., *Crystal structures of 7-methylguanosine 5'-triphosphate (m(7)GTP)- and P(1)-7-methylguanosine-P(3)-adenosine-5',5'-triphosphate (m(7)GpppA)-bound human full-length eukaryotic initiation factor 4E: biological importance of the C-terminal flexible region*. Biochem J, 2002. **362**(Pt 3): p. 539-44.
78. Pause, A., et al., *Insulin-dependent stimulation of protein synthesis by phosphorylation of a regulator of 5'-cap function*. Nature, 1994. **371**(6500): p. 762-7.
79. Gingras, A.C., et al., *Regulation of 4E-BP1 phosphorylation: a novel two-step mechanism*. Genes Dev, 1999. **13**(11): p. 1422-37.
80. Gingras, A.C., et al., *Hierarchical phosphorylation of the translation inhibitor 4E-BP1*. Genes Dev, 2001. **15**(21): p. 2852-64.
81. Gradi, A., et al., *A novel functional human eukaryotic translation initiation factor 4G*. Mol Cell Biol, 1998. **18**(1): p. 334-42.
82. Pyronnet, S., et al., *Human eukaryotic translation initiation factor 4G (eIF4G) recruits mnk1 to phosphorylate eIF4E*. Embo j, 1999. **18**(1): p. 270-9.
83. Imataka, H., A. Gradi, and N. Sonenberg, *A newly identified N-terminal amino acid sequence of human eIF4G binds poly(A)-binding protein and functions in poly(A)-dependent translation*. Embo j, 1998. **17**(24): p. 7480-9.
84. Gallie, D.R., *The cap and poly(A) tail function synergistically to regulate mRNA translational efficiency*. Genes Dev, 1991. **5**(11): p. 2108-16.
85. Hilbert, M., et al., *eIF4G stimulates the activity of the DEAD box protein eIF4A by a conformational guidance mechanism*. Nucleic acids research, 2010. **39**: p. 2260-70.
86. Marcotrigiano, J., et al., *A conserved HEAT domain within eIF4G directs assembly of the translation initiation machinery*. Mol Cell, 2001. **7**(1): p. 193-203.
87. Imataka, H. and N. Sonenberg, *Human eukaryotic translation initiation factor 4G (eIF4G) possesses two separate and independent binding sites for eIF4A*. Mol Cell Biol, 1997. **17**(12): p. 6940-7.
88. Marintchev, A., et al., *Topology and regulation of the human eIF4A/4G/4H helicase complex in translation initiation*. Cell, 2009. **136**(3): p. 447-60.

89. Pyronnet, S., et al., *Human eukaryotic translation initiation factor 4G (eIF4G) recruits mnk1 to phosphorylate eIF4E*. The EMBO journal, 1999. **18**(1): p. 270-279.
90. Linder, P. and E. Jankowsky, *From unwinding to clamping — the DEAD box RNA helicase family*. Nature Reviews Molecular Cell Biology, 2011. **12**(8): p. 505-516.
91. Rogers, G.W., Jr., A.A. Komar, and W.C. Merrick, *eIF4A: the godfather of the DEAD box helicases*. Prog Nucleic Acid Res Mol Biol, 2002. **72**: p. 307-31.
92. Chan, C.C., et al., *eIF4A3 is a novel component of the exon junction complex*. Rna, 2004. **10**(2): p. 200-9.
93. Ferraiuolo, M.A., et al., *A nuclear translation-like factor eIF4AIII is recruited to the mRNA during splicing and functions in nonsense-mediated decay*. Proc Natl Acad Sci U S A, 2004. **101**(12): p. 4118-23.
94. Shibuya, T., et al., *eIF4AIII binds spliced mRNA in the exon junction complex and is essential for nonsense-mediated decay*. Nat Struct Mol Biol, 2004. **11**(4): p. 346-51.
95. Galicia-Vázquez, G., et al., *A cellular response linking eIF4AI activity to eIF4AII transcription*. Rna, 2012. **18**(7): p. 1373-84.
96. Laschober, G.T., et al., *Identification of evolutionarily conserved genetic regulators of cellular aging*. Aging Cell, 2010. **9**(6): p. 1084-97.
97. Williams-Hill, D.M., et al., *Differential expression of the murine eukaryotic translation initiation factor isoforms eIF4A(I) and eIF4A(II) is dependent upon cellular growth status*. Arch Biochem Biophys, 1997. **338**(1): p. 111-20.
98. García-García, C., et al., *RNA BIOCHEMISTRY. Factor-dependent processivity in human eIF4A DEAD-box helicase*. Science, 2015. **348**(6242): p. 1486-8.
99. Peck, M.L. and D. Herschlag, *Effects of oligonucleotide length and atomic composition on stimulation of the ATPase activity of translation initiation factor eIF4A*. Rna, 1999. **5**(9): p. 1210-21.
100. Sen, N.D., et al., *eIF4B stimulates translation of long mRNAs with structured 5' UTRs and low closed-loop potential but weak dependence on eIF4G*. Proceedings of the National Academy of Sciences, 2016. **113**(38): p. 10464-10472.
101. Feoktistova, K., et al., *Human eIF4E promotes mRNA restructuring by stimulating eIF4A helicase activity*. Proceedings of the National Academy of Sciences, 2013. **110**(33): p. 13339-13344.
102. Chang, J.H., et al., *Crystal structure of the eIF4A-PDCD4 complex*. Proceedings of the National Academy of Sciences, 2009. **106**(9): p. 3148-3153.
103. LaRonde-LeBlanc, N., et al., *Structural basis for inhibition of translation by the tumor suppressor Pcd4*. Mol Cell Biol, 2007. **27**(1): p. 147-56.
104. Cai, W., et al., *Wanted DEAD/H or Alive: Helicases Winding Up in Cancers*. JNCI: Journal of the National Cancer Institute, 2017. **109**(6).
105. Fuller-Pace, F.V., *DEAD box RNA helicase functions in cancer*. RNA Biology, 2013. **10**(1): p. 121-132.
106. Robert, F. and J. Pelletier, *Perturbations of RNA helicases in cancer*. Wiley Interdiscip Rev RNA, 2013. **4**(4): p. 333-49.

107. Fuller-Pace, F.V., *DEAD box RNA helicase functions in cancer*. RNA Biol, 2013. **10**(1): p. 121-32.
108. Schalm, S.S., et al., *TOS motif-mediated raptor binding regulates 4E-BP1 multisite phosphorylation and function*. Curr Biol, 2003. **13**(10): p. 797-806.
109. Wendel, H.-G., et al., *Survival signalling by Akt and eIF4E in oncogenesis and cancer therapy*. Nature, 2004. **428**(6980): p. 332-337.
110. Lazaris-Karatzas, A., K.S. Montine, and N. Sonenberg, *Malignant transformation by a eukaryotic initiation factor subunit that binds to mRNA 5' cap*. Nature, 1990. **345**(6275): p. 544-547.
111. Dorrello, N.V., et al., *S6K1- and TRCP-Mediated Degradation of PDCD4 Promotes Protein Translation and Cell Growth*. Science, 2006. **314**(5798): p. 467-471.
112. Sanchez-Vega, F., et al., *Oncogenic Signaling Pathways in The Cancer Genome Atlas*. Cell, 2018. **173**(2): p. 321-337.e10.
113. Vikhreva, P.N., S.V. Kalinichenko, and I.V. Korobko, *Programmed cell death 4 mechanism of action: The model to be updated?* Cell Cycle, 2017. **16**(19): p. 1761-1764.
114. Bhat, M., et al., *Targeting the translation machinery in cancer*. Nat Rev Drug Discov, 2015. **14**(4): p. 261-78.
115. Parsyan, A., et al., *mRNA helicases: the tacticians of translational control*. Nature Reviews Molecular Cell Biology, 2011. **12**(4): p. 235-245.
116. Botlagunta, M., et al., *Oncogenic role of DDX3 in breast cancer biogenesis*. Oncogene, 2008. **27**(28): p. 3912-3922.
117. Kim, K.-A., et al., *Mitogenic influence of human R-spondin1 on the intestinal epithelium*. Science, 2005. **309**(5738): p. 1256-1259.
118. Sun, M., et al., *The role of DDX3 in regulating Snail*. Biochimica et Biophysica Acta (BBA)-Molecular Cell Research, 2011. **1813**(3): p. 438-447.
119. Sun, M., et al., *DDX3 regulates DNA damage-induced apoptosis and p53 stabilization*. Biochimica et Biophysica Acta (BBA)-Molecular Cell Research, 2013. **1833**(6): p. 1489-1497.
120. Huusko, P., et al., *Nonsense-mediated decay microarray analysis identifies mutations of EPHB2 in human prostate cancer*. Nature Genetics, 2004. **36**(9): p. 979-983.
121. Saporita, A.J., et al., *RNA helicase DDX5 is a p53-independent target of ARF that participates in ribosome biogenesis*. Cancer Res, 2011. **71**(21): p. 6708-17.
122. Novac, O., A.S. Guenier, and J. Pelletier, *Inhibitors of protein synthesis identified by a high throughput multiplexed translation screen*. Nucleic Acids Res, 2004. **32**(3): p. 902-15.
123. Chen, W.H., S.K. Wang, and C.Y. Duh, *Polyhydroxylated steroids from the bamboo coral *Isis hippuris**. Mar Drugs, 2011. **9**(10): p. 1829-1839.
124. Rust, M., et al., *A multiproducer microbiome generates chemical diversity in the marine sponge *Mycale hentscheli**. Proceedings of the National Academy of Sciences, 2020. **117**(17): p. 9508-9518.

125. Müller, C., et al., *Broad-spectrum antiviral activity of the eIF4A inhibitor silvestrol against corona- and picornaviruses*. Antiviral Res, 2018. **150**: p. 123-129.
126. Chao, C.H., et al., *Polyoxygenated steroids from the gorgonian Isis hippuris*. J Nat Prod, 2005. **68**(6): p. 880-5.
127. Lindqvist, L., et al., *Selective pharmacological targeting of a DEAD box RNA helicase*. PLoS One, 2008. **3**(2): p. e1583.
128. Sun, Y., et al., *Single-molecule kinetics of the eukaryotic initiation factor 4A1 upon RNA unwinding*. Structure, 2014. **22**(7): p. 941-8.
129. Cencic, R. and J. Pelletier, *Hippuristanol - A potent steroid inhibitor of eukaryotic initiation factor 4A*. Translation (Austin), 2016. **4**(1): p. e1137381.
130. Bordeleau, M.-E., et al., *Functional characterization of IRESes by an inhibitor of the RNA helicase eIF4A*. Nature chemical biology, 2006. **2**(4): p. 213-220.
131. Steinberger, J., et al., *Identification and characterization of hippuristanol-resistant mutants reveals eIF4A1 dependencies within mRNA 5' leader regions*. Nucleic Acids Research, 2020. **48**(17): p. 9521-9537.
132. Ishikawa, C., et al., *Hippuristanol reduces the viability of primary effusion lymphoma cells both in vitro and in vivo*. Marine drugs, 2013. **11**(9): p. 3410-3424.
133. Tsumuraya, T., et al., *Effects of hippuristanol, an inhibitor of eIF4A, on adult T-cell leukemia*. Biochemical pharmacology, 2011. **81**(6): p. 713-722.
134. Cencic, R., et al., *Modifying chemotherapy response by targeted inhibition of eukaryotic initiation factor 4A*. Blood cancer journal, 2013. **3**(7): p. e128-e128.
135. Robert, F., et al., *Translation initiation factor eIF4F modifies the dexamethasone response in multiple myeloma*. Proceedings of the National Academy of Sciences, 2014. **111**(37): p. 13421-13426.
136. Northcote, P.T., J.W. Blunt, and M.H.G. Munro, *Pateamine: a potent cytotoxin from the New Zealand Marine sponge, mycale sp.* Tetrahedron Letters, 1991. **32**(44): p. 6411-6414.
137. Low, W.K., et al., *Inhibition of eukaryotic translation initiation by the marine natural product pateamine A*. Mol Cell, 2005. **20**(5): p. 709-22.
138. Bordeleau, M.E., et al., *RNA-mediated sequestration of the RNA helicase eIF4A by Pateamine A inhibits translation initiation*. Chem Biol, 2006. **13**(12): p. 1287-95.
139. Romo, D., et al., *Evidence for separate binding and scaffolding domains in the immunosuppressive and antitumor marine natural product, pateamine a: design, synthesis, and activity studies leading to a potent simplified derivative*. J Am Chem Soc, 2004. **126**(34): p. 10582-8.
140. Kuznetsov, G., et al., *Potent in vitro and in vivo anticancer activities of des-methyl, des-amino pateamine A, a synthetic analogue of marine natural product pateamine A*. Mol Cancer Ther, 2009. **8**(5): p. 1250-60.
141. Lu King, M., et al., *X-Ray crystal structure of rocaglamide, a novel antileukemic 1H-cyclopenta[b]benzofuran from Aglaia elliptifolia*. Journal of the Chemical Society, Chemical Communications, 1982(20): p. 1150-1151.

142. Bordeleau, M.-E., et al., *Therapeutic suppression of translation initiation modulates chemosensitivity in a mouse lymphoma model*. The Journal of clinical investigation, 2008. **118**(7): p. 2651-2660.
143. Rozen, F., et al., *Bidirectional RNA helicase activity of eucaryotic translation initiation factors 4A and 4F*. Mol Cell Biol, 1990. **10**(3): p. 1134-44.
144. Rubio, C.A., et al., *Transcriptome-wide characterization of the eIF4A signature highlights plasticity in translation regulation*. Genome Biology, 2014. **15**(10): p. 476.
145. Chu, J., et al., *Rocaglates Induce Gain-of-Function Alterations to eIF4A and eIF4F*. Cell Rep, 2020. **30**(8): p. 2481-2488.e5.
146. Chu, J., et al., *CRISPR-Mediated Drug-Target Validation Reveals Selective Pharmacological Inhibition of the RNA Helicase, eIF4A*. Cell Rep, 2016. **15**(11): p. 2340-7.
147. Iwasaki, S., et al., *The Translation Inhibitor Rocaglamide Targets a Bimolecular Cavity between eIF4A and Polypurine RNA*. Mol Cell, 2019. **73**(4): p. 738-748.e9.
148. Zhang, W., et al., *Intercepted Retro-Nazarov Reaction: Syntheses of Amidino-Rocaglate Derivatives and Their Biological Evaluation as eIF4A Inhibitors*. Journal of the American Chemical Society, 2019. **141**(32): p. 12891-12900.
149. Cencic, R., et al., *Antitumor activity and mechanism of action of the cyclopenta [b] benzofuran, silvestrol*. PloS one, 2009. **4**(4): p. e5223.
150. Lin, T.C., *DDX3X Multifunctionally Modulates Tumor Progression and Serves as a Prognostic Indicator to Predict Cancer Outcomes*. Int J Mol Sci, 2019. **21**(1).
151. Stransky, N., et al., *The Mutational Landscape of Head and Neck Squamous Cell Carcinoma*. Science, 2011. **333**(6046): p. 1157-1160.
152. Alkallas, R., et al., *Multi-omic analysis reveals significantly mutated genes and DDX3X as a sex-specific tumor suppressor in cutaneous melanoma*. Nature Cancer, 2020. **1**(6): p. 635-652.
153. Ariumi, Y., *Multiple functions of DDX3 RNA helicase in gene regulation, tumorigenesis, and viral infection*. Front Genet, 2014. **5**: p. 423.
154. Maga, G., et al., *Pharmacophore Modeling and Molecular Docking Led to the Discovery of Inhibitors of Human Immunodeficiency Virus-1 Replication Targeting the Human Cellular Aspartic Acid–Glutamic Acid–Alanine–Aspartic Acid Box Polypeptide 3*. Journal of Medicinal Chemistry, 2008. **51**(21): p. 6635-6638.
155. Yedavalli, V.S.R.K., et al., *Ring Expanded Nucleoside Analogues Inhibit RNA Helicase and Intracellular Human Immunodeficiency Virus Type 1 Replication*. Journal of Medicinal Chemistry, 2008. **51**(16): p. 5043-5051.
156. Bol, G.M., et al., *Targeting DDX3 with a small molecule inhibitor for lung cancer therapy*. EMBO Mol Med, 2015. **7**(5): p. 648-69.
157. Wilky, B.A., et al., *RNA helicase DDX3: a novel therapeutic target in Ewing sarcoma*. Oncogene, 2016. **35**(20): p. 2574-2583.

158. Samal, S.K., et al., *Ketorolac salt is a newly discovered DDX3 inhibitor to treat oral cancer*. Scientific Reports, 2015. **5**(1): p. 9982.
159. Chen, M., et al., *Dual targeting of DDX3 and eIF4A by the translation inhibitor rocaglamide A*. Cell Chem Biol, 2021. **28**(4): p. 475-486.e8.
160. Xing, Z., W.K. Ma, and E.J. Tran, *The DDX5/Dbp2 subfamily of DEAD-box RNA helicases*. Wiley Interdiscip Rev RNA, 2019. **10**(2): p. e1519.
161. Kost, G.C., et al., *A Novel Anti-Cancer Agent, 1-(3,5-Dimethoxyphenyl)-4-[(6-Fluoro-2-Methoxyquinoxalin-3-yl)Aminocarbonyl] Piperazine (RX-5902), Interferes With β -Catenin Function Through Y593 Phospho-p68 RNA Helicase*. J Cell Biochem, 2015. **116**(8): p. 1595-601.
162. Capasso, A., et al., *First-in-Class Phosphorylated-p68 Inhibitor RX-5902 Inhibits β -Catenin Signaling and Demonstrates Antitumor Activity in Triple-Negative Breast Cancer*. Mol Cancer Ther, 2019. **18**(11): p. 1916-1925.
163. Tentler, J.J., et al., *RX-5902, a novel β -catenin modulator, potentiates the efficacy of immune checkpoint inhibitors in preclinical models of triple-negative breast Cancer*. BMC Cancer, 2020. **20**(1): p. 1063.
164. Supek, F., B. Lehner, and R.G.H. Lindeboom, *To NMD or Not To NMD: Nonsense-Mediated mRNA Decay in Cancer and Other Genetic Diseases*. Trends in Genetics, 2021. **37**(7): p. 657-668.
165. Cencic, R., et al., *CRISPR-Based Screen Links an Inhibitor of Nonsense-Mediated Decay to eIF4A3 Target Engagement*. ACS Chemical Biology, 2020. **15**(6): p. 1621-1629.
166. Mizojiri, R., et al., *Discovery of Novel 5-(Piperazine-1-carbonyl)pyridin-2(1H)-one Derivatives as Orally eIF4A3-Selective Inhibitors*. ACS Medicinal Chemistry Letters, 2017. **8**(10): p. 1077-1082.
167. Lorsch, J.R. and D. Herschlag, *The DEAD Box Protein eIF4A. 1. A Minimal Kinetic and Thermodynamic Framework Reveals Coupled Binding of RNA and Nucleotide*. Biochemistry, 1998. **37**(8): p. 2180-2193.
168. Langlais, D., et al., *Rocaglates as dual-targeting agents for experimental cerebral malaria*. Proceedings of the National Academy of Sciences, 2018. **115**(10): p. E2366-E2375.
169. Grifo, J.A., et al., *RNA-stimulated ATPase activity of eukaryotic initiation factors*. J Biol Chem, 1984. **259**(13): p. 8648-54.
170. Rogers, G.W., Jr., N.J. Richter, and W.C. Merrick, *Biochemical and kinetic characterization of the RNA helicase activity of eukaryotic initiation factor 4A*. J Biol Chem, 1999. **274**(18): p. 12236-44.
171. Abramson, R.D., et al., *The ATP-dependent interaction of eukaryotic initiation factors with mRNA*. J Biol Chem, 1987. **262**(8): p. 3826-32.
172. Chu, J., et al., *Amidino-Rocaglates: A Potent Class of eIF4A Inhibitors*. Cell Chem Biol, 2019. **26**(11): p. 1586-1593.e3.
173. Iwasaki, S., S.N. Floor, and N.T. Ingolia, *Rocaglates convert DEAD-box protein eIF4A into a sequence-selective translational repressor*. Nature, 2016. **534**(7608): p. 558-561.
174. Naineni, S.K., et al., *Functional mimicry revealed by the crystal structure of an eIF4A:RNA complex bound to the interfacial inhibitor, desmethyl pateamine A*. Cell Chem Biol, 2021. **28**(6): p. 825-834.e6.

175. Abdelhaleem, M., L. Maltais, and H. Wain, *The human DDX and DHX gene families of putative RNA helicases*. Genomics, 2003. **81**(6): p. 618-622.
176. van Voss, M.R.H., et al., *DDX3 has divergent roles in head and neck squamous cell carcinomas in smoking vs non-smoking patients*. DDX3 in cancer, 2017: p. 137.
177. Arora, A., et al., *RECQL4 helicase has oncogenic potential in sporadic breast cancers*. The Journal of pathology, 2016. **238**(4): p. 495-501.
178. Dhar, S., A. Datta, and R.M. Brosh, *DNA helicases and their roles in cancer*. DNA Repair, 2020. **96**: p. 102994.
179. Maity, J., et al., *Targeting of RecQ Helicases as a Novel Therapeutic Strategy for Ovarian Cancer*. Cancers, 2022. **14**(5): p. 1219.
180. Ellis, N.A., et al., *The Bloom's syndrome gene product is homologous to RecQ helicases*. Cell, 1995. **83**(4): p. 655-666.
181. Yu, C.-E., et al., *Positional cloning of the Werner's syndrome gene*. Science, 1996. **272**(5259): p. 258-262.
182. Kitao, S., et al., *Mutations in RECQL4 cause a subset of cases of Rothmund-Thomson syndrome*. Nature genetics, 1999. **22**(1): p. 82-84.
183. Brosh, R.M., *DNA helicases involved in DNA repair and their roles in cancer*. Nature Reviews Cancer, 2013. **13**(8): p. 542-558.
184. Moser, R., et al., *MYC-Driven Tumorigenesis Is Inhibited by WRN Syndrome Gene Deficiency Werner Deficiency Impairs Myc-Induced Tumorigenesis*. Molecular Cancer Research, 2012. **10**(4): p. 535-545.
185. Aggarwal, M., et al., *Inhibition of helicase activity by a small molecule impairs Werner syndrome helicase (WRN) function in the cellular response to DNA damage or replication stress*. Proceedings of the National Academy of Sciences, 2011. **108**(4): p. 1525-1530.
186. Datta, A. and R.M. Brosh, Jr., *New Insights Into DNA Helicases as Druggable Targets for Cancer Therapy*. Front Mol Biosci, 2018. **5**: p. 59.
187. Newman, Joseph A. and O. Gileadi, *RecQ helicases in DNA repair and cancer targets*. Essays in Biochemistry, 2020. **64**(5): p. 819-830.
188. Godbout, R. and J. Squire, *Amplification of a DEAD box protein gene in retinoblastoma cell lines*. Proceedings of the National Academy of Sciences, 1993. **90**(16): p. 7578-7582.
189. George, R., et al., *Analysis of candidate gene co-amplification with MYCN in neuroblastoma*. European Journal of Cancer, 1997. **33**(12): p. 2037-2042.
190. George, R.E., et al., *Investigation of co-amplification of the candidate genes ornithine decarboxylase, ribonucleotide reductase, syndecan-1 and a DEAD box gene, DDX1, with N-myc in neuroblastoma*. United Kingdom Children's Cancer Study Group. Oncogene, 1996. **12**(7): p. 1583-1587.
191. Manohar, C.F., et al., *Co-amplification and concomitant high levels of expression of a DEAD box gene with MYCN in human neuroblastoma*. Genes, Chromosomes and Cancer, 1995. **14**(3): p. 196-203.
192. Squire, J.A., et al., *Co-amplification of MYCN and a DEAD box gene (DDX1) in primary neuroblastoma*. Oncogene, 1995. **10**(7): p. 1417-1422.

193. Hodgson, J.G., et al., *Comparative analyses of gene copy number and mRNA expression in glioblastoma multiforme tumors and xenografts*. *Neuro-oncology*, 2009. **11**(5): p. 477-487.
194. Chen, H.-H., et al., *DDX3 activates CBC-eIF3-mediated translation of uORF-containing oncogenic mRNAs to promote metastasis in HNSCC*. *Cancer research*, 2018. **78**(16): p. 4512-4523.
195. Bol, G.M., et al., *Targeting DDX 3 with a small molecule inhibitor for lung cancer therapy*. *EMBO molecular medicine*, 2015. **7**(5): p. 648-669.
196. Bol, G.M., et al., *Expression of the RNA helicase DDX3 and the hypoxia response in breast cancer*. *PloS one*, 2013. **8**(5): p. e63548.
197. Hueng, D.-Y., et al., *DDX3X biomarker correlates with poor survival in human gliomas*. *International journal of molecular sciences*, 2015. **16**(7): p. 15578-15591.
198. Liang, S., et al., *The clinical and pathological significance of Nectin-2 and DDX3 expression in pancreatic ductal adenocarcinomas*. *Disease Markers*, 2015. **2015**.
199. Miao, X., et al., *Nectin-2 and DDX3 are biomarkers for metastasis and poor prognosis of squamous cell/adenosquamous carcinomas and adenocarcinoma of gallbladder*. *International journal of clinical and experimental pathology*, 2013. **6**(2): p. 179.
200. Le Quesne, J.P., et al., *Dysregulation of protein synthesis and disease*. *J Pathol*, 2010. **220**(2): p. 140-51.
201. Scheper, G.C., M.S. van der Knaap, and C.G. Proud, *Translation matters: protein synthesis defects in inherited disease*. *Nature Reviews Genetics*, 2007. **8**(9): p. 711-723.
202. Yángüez, E., et al., *Functional impairment of eIF4A and eIF4G factors correlates with inhibition of influenza virus mRNA translation*. *Virology*, 2011. **413**(1): p. 93-102.
203. Hosmillo, M., et al., *The RNA Helicase eIF4A Is Required for Sapovirus Translation*. *Journal of Virology*, 2016. **90**(10): p. 5200-5204.
204. Surakasi, V.P., M. Nalini, and Y. Kim, *Host translational control of a polydnavirus, Cotesia plutellae bracovirus, by sequestering host eIF4A to prevent formation of a translation initiation complex*. *Insect Molecular Biology*, 2011. **20**(5): p. 609-618.
205. Faller, W.J., et al., *mTORC1-mediated translational elongation limits intestinal tumour initiation and growth*. *Nature*, 2015. **517**(7535): p. 497-500.
206. Wolfe, A.L., et al., *RNA G-quadruplexes cause eIF4A-dependent oncogene translation in cancer*. *Nature*, 2014. **513**(7516): p. 65-70.
207. Verma, M., et al., *A short translational ramp determines the efficiency of protein synthesis*. *Nat Commun*, 2019. **10**(1): p. 5774.
208. Malka-Mahieu, H., et al., *Molecular Pathways: The eIF4F Translation Initiation Complex-New Opportunities for Cancer Treatment*. *Clin Cancer Res*, 2017. **23**(1): p. 21-25.
209. Bordeleau, M.-E., et al., *Stimulation of mammalian translation initiation factor eIF4A activity by a small molecule inhibitor of eukaryotic translation*. *Proceedings of the National Academy of Sciences*, 2005. **102**(30): p. 10460-10465.

210. Alqahtani, H., et al., *DDX17 (P72), a Sox2 binding partner, promotes stem-like features conferred by Sox2 in a small cell population in estrogen receptor-positive breast cancer*. Cellular signalling, 2016. **28**(2): p. 42-50.
211. Li, K., et al., *Upregulated expression of DDX5 predicts recurrence and poor prognosis in breast cancer*. Pathology-Research and Practice, 2022. **229**: p. 153736.
212. Li, K., et al., *DDX17 nucleocytoplasmic shuttling promotes acquired gefitinib resistance in non-small cell lung cancer cells via activation of β -catenin*. Cancer letters, 2017. **400**: p. 194-202.
213. Wu, X.-C., et al., *Long noncoding RNA SNHG20 promotes prostate cancer progression via upregulating DDX17*. Archives of Medical Science: AMS, 2021. **17**(6): p. 1752.
214. Liu, C., et al., *Hepatoma-derived growth factor and DDX5 promote carcinogenesis and progression of endometrial cancer by activating β -catenin*. Frontiers in oncology, 2019. **9**: p. 211.
215. Dai, L., et al., *High expression of ALDOA and DDX5 are associated with poor prognosis in human colorectal cancer*. Cancer Management and Research, 2018. **10**: p. 1799.
216. Fu, Q., et al., *miRomics and Proteomics Reveal a miR-296-3p/PRKCA/FAK/Ras/c-Myc Feedback Loop Modulated by HDGF/DDX5/ β -catenin Complex in Lung Adenocarcinoma miR-296-3p/PRKCA/c-Myc Circuit Modulated by HDGF/DDX5*. Clinical Cancer Research, 2017. **23**(20): p. 6336-6350.
217. Ma, Z., et al., *Knockdown of DDX5 inhibits the proliferation and tumorigenesis in esophageal cancer*. Oncology Research, 2017. **25**(6): p. 887.
218. Wu, N., et al., *miR-5590-3p inhibited tumor growth in gastric cancer by targeting DDX5/AKT/m-TOR pathway*. Biochemical and biophysical research communications, 2018. **503**(3): p. 1491-1497.
219. Wang, R., et al., *P68 RNA helicase promotes invasion of glioma cells through negatively regulating DUSP5*. Cancer science, 2019. **110**(1): p. 107-117.
220. Qing, S., et al., *Proteomic identification of potential biomarkers for cervical squamous cell carcinoma and human papillomavirus infection*. Tumor Biology, 2017. **39**(4): p. 1010428317697547.
221. Xue, Y., et al., *DDX17 promotes hepatocellular carcinoma progression via inhibiting Klf4 transcriptional activity*. Cell death & disease, 2019. **10**(11): p. 1-11.
222. Luo, Q., et al., *Upregulation of DEAD box helicase 5 and 17 are correlated with the progression and poor prognosis in gliomas*. Pathology-Research and Practice, 2020. **216**(3): p. 152828.